2021

Develop Biochar-based Controlled Release Nitrogen Fertilizers

Zhisheng Cen
South Dakota State University

DEVELOP BIOCHAR-BASED CONTROLLED RELEASE NITROGEN FERTILIZERS

BY

ZHISHENG CEN

A thesis submitted in partial fulfillment of the requirements for the

Master of Science

Major in Agricultural and Biosystems engineering

South Dakota State University

2021

THESIS ACCEPTANCE PAGE

Zhisheng Cen

This thesis is approved as a creditable and independent investigation by a candidate for the master's degree and is acceptable for meeting the thesis requirements for this degree. Acceptance of this does not imply that the conclusions reached by the candidate are necessarily the conclusions of the major department.

Lin Wei
Advisor Date

Van Kelley
Department Head Date

Nicole Lounsbery, PhD
Director, Graduate School Date

ACKNOWLEDGEMENTS

I would like to express my greatest gratitude to my advisor Dr. Lin Wei. During the past two years, Dr. Wei encouraged me to tackle the challenges I encountered in research and guided me to solve problems independently. His strict requirement and rigorous academic attitude resulted in a big progress in my research. He gave me many heuristic instructions on biochar and controlled release fertilizer research. I learned a lot from him about how to manage lab works and do research efficiently.

I would like to thank Dr. Kasiviswanathan Muthukumarappan for his valuable instructions and suggestions during my master study. I also want to thank Dr. Xufei Yang for sharing with me his work and academic experiences; to Dr. Cheng Zhang for his guidance and suggestions for my research; to Dr. Gary Anderson for his advice on how to study and sharing American life and experiences. Special thanks are also given to Dr. Yajun Wu for his guidance and advice for the greenhouse experiments, and the introduction to the plant biology field.

I'm grateful to my colleagues Mr. Abdus Sobhan and Mr. Shun Lu for their support and kind help. Our struggling and happy days are unforgettable. I thank undergraduate research assistant Madison Best for her contribution to the research of biochar-films.

I would like to express my deep appreciation and love to my parents. Their support and love are the biggest encouragement for me to overcome all the challenges in my study as well as in my life.

Lastly, I want to thank all the faculty at SDSU. Because of them, my past two years of experience at SDSU is one of the most important parts in my life.

CONTENTS

ABBREVIATIONS

AC	Activated carbon
AB	Activated biochar
ACRNF	Asphalt-based controlled release nitrogenous fertilizer
BC	Biochar
BCRNF	Biochar-based controlled released nitrogenous fertilizer
BNF	Biochar-based nitrogenous fertilizer
CNC	Cellulose nanocrystal
CNF	Cellulose nanofibril
CRF	Controlled release fertilizer
MB	Methylene blue
N	Nitrogen
N-P-K	Nitrogen-phosphorus-potassium
PLA	Polylactic acid
SA	Sodium Alginate
SEM	Scanning Electron Microscope

LIST OF FIGURES

LIST OF TABLES

ABSTRACT

DEVELOP BIOCHAR-BASED CONTROLLED RELEASE NITROGEN FERTILIZER

ZHISHENG CEN

2021

The current efficiency of conventional nitrogenous fertilizers (e.g. urea, ammonium sulfate, etc.) in agricultural practices is low, fluctuating from 30 to 40%. Approximately 60% of nitrogenous fertilizers were wasted due to vaporization into the air, runoff or leaching into water systems. The lost nitrogen (N) resulted in not only high production cost but also serious environmental problems, such as greenhouse gas (N_2O) emission in the atmosphere, algal blooms, oxygen depletion, fish kills, and loss of biodiversity in surface water due to eutrophication or pollution. To address these problems, this study aimed to utilize low-cost biochar-based materials to develop a controllable, affordable, and environmentally friendly nitrogen fertilizer. The studies of activated biochar, biochar-based controlled release nitrogenous fertilizer (BCRNF), and asphalt-based controlled release nitrogenous fertilizer (ACRNF) were carried out to achieve the goal.

To improve the adsorption ability of biochar, biochar was activated by steam-method. After steam-activation, activated biochar (AB) has attained approximate methylene blue (MB) adsorption with activated carbon (AC). Besides, the film produced in this study by AB and cellulose nanofibrils has formed a stable form, promising to part of BCRNF in the future.

To attain a controllable and endurable N-release pattern, polylactic acid (PLA), that, has a strong hydrophobic property, and biochar that possesses, a strong adsorption capability, were chosen as coating material and N carrier respectively to prepare BCRNF.

In BCRNFs' N-release in water experiment, BCRNF-P10 continually released N in water in 12 days. In the soil column leaching experiment, for BCRNF-P10 sample, it continually released N for 25 days and only 33.57% of N was leached into water under a rainy simulated environment. These results indicate that the BCRNF has the potential for developing controlled release nitrogen fertilizer in the future.

To attain a more durable N-release pattern, another biochar-based nitrogen fertilizer, asphalt-based controlled release nitrogenous fertilizer (ACRNF) was developed. The asphalt used as N carrier in the fabrication of ACRNF was produced from bio-based materials: corn stover and sawdust by pyrolysis and liquefication, respectively. Granular ammonium sulfate was either mixed or coated with asphalt to control N-release. Different ACRNF samples were tested to examine their N-release in water. The results showed that the N-release patterns of ACRNF were significantly different when ammonium sulfate particles were mixed or coated with asphalt under different processing conditions. The N-release time of 80% N for the sample ACRNF 230 was more than 20 days. The performance of other ACRNF samples also demonstrated the concept of controllable N-release if ammonium sulfate was properly mixing or coating with asphalt. Although further research is needed, the ACRNF has shown very promising potential to improve nitrogen use efficiency in corn production in the controlled release fertilizer market.

CHAPTER 1: INTRODUCTION

1.1 Background

The yields of many crops (e.g. corn, wheat, rice) heavily rely on nitrogen (N) fertilizers such as urea, ammonium sulfate, etc. The economic research service of USDA reported that the consumption of N fertilizers was more than 27 million tons in the US in 2015 [1]. It is estimated that the consumption of N will be continually growing due to food security for the rapidly escalating global population. However, the current efficiency of these conventional N fertilizers (e.g. urea, ammonium sulfate, etc.) in agricultural practices is low, fluctuating from 30 to 40%. Approximately 60% of N fertilizers were wasted due to vaporization into the air, runoff, or leaching into water systems [2]. The low efficiency of N fertilizer has resulted in not only high production cost but also serious environmental problems, such as greenhouse gas (N_2O) emission in the atmosphere, algal blooms, oxygen depletion, fish kills, loss of biodiversity in surface water due to eutrophication or pollution [3].

1.2 Controlled release fertilizers (CRFs)

To address these issues, many researchers have tried to develop various controlled release fertilizers (CRFs) to improve nitrogen use efficiency [4]. The goal of CRFs is to achieve predictable and controllable N released patterns to meet the demand for crop growth. The demand for N nutrient varies significantly during different growth stages. For example, a corn plant needs very little N (< 0.5 lb/acre per day) in the first 3 weeks after seeding. But after the 3 weeks, the corn plant takes up exponentially more N until

the 8th week, with an average of 3.3 lb/acre per day and highest uptake of 5.4 lb/acre per day. More than 70% of N uptake occurs within 25 – 30 days of the middle vegetative stage (between the 4th week and the 8th week), and then much less N (< 0.6 lb/acre per day) is needed in the later period of reproductive to mature stages [5-12]. Currently, the practice of fertilization is poor synchrony between the N application and corn growing demand. About 75% of N fertilizer applications are made before planting in the US [9-13]. Most of the N fertilizers applied are instantly dissolving in water or bursting release into the soil. The timing of N availability doesn't match the demand for corn growth. The time between N application and its active uptake by the corn provides numerous opportunities for N loss from leaching, clay fixation, immobilization, denitrification, and volatilization. The N applied may be lost to the groundwater through leaching or is then transported to the nearby surface waters via surface runoff or directly via tile drainage bypassing stream buffer [12 – 14]. Besides, significant fractions of the applied N are lost into the air through the emission of ammonia (NH_3), nitrous oxide (N_2O), and nitric oxide (NO). The NH_3 emission contributes to water eutrophication and land acidification when redeposited on the earth's surface through the rain. The N2O is a potent greenhouse gas and plays a key role in tropospheric ozone chemistry [15-17]. To increase N availability and accessibility, multiple applications of N fertilizers are being applied in a single growing season by heavily machine systems along with high labor costs in the US. This directly results in low efficiency and high production costs.

To improve N availability and accessibility for timely crop uptake while minimizing nutrient loss, fertilization should meet the 4Rs of stewardship: right source, right rate, right time, and the right place. CRFs should be designed for the timely release of N into

the soil at the desired rate, pattern, and duration to synchronize the demand for crop growth. Ideally, the N-release rate, time, and pattern of CRF are predictable and controllable to meet the N demand of crop growth for the entire season through a single application to reduce the fertilizer consumption and labor cost. Since the first CRF, in which the fertilizer was coated with sulfur and polyethylene to control N release, was commercially available in the 1960s, many progresses have been made in CRF's design and production. Currently, market available CRFs were mainly produced by two different technologies: 1) N fertilizers mixed with a matrix of low-solubility compound (either organic or inorganic). The N release pattern is controlled by water solubility of the CRF mixture; 2) N fertilizers were coated with a physical barrier of the coating layer, either hydrophobic (e.g. olefin, rubber) or hydrophilic (e.g. thermoplastics, resins). The N releasing is depending on the material type and microstructure of the coating layer [18]. The global CRF market was worth $1.45 billion in 2018 and was estimated to reach a valuation of $2.35 billion by the end of 2024 [19-20]. Nonetheless, the high cost is the most prominent obstacle for CRF application. Due to expensive coating materials and complicated production processes, the prices of existing CRFs are several times higher than that of conventional N fertilizers, limiting their use to only high cash crops or specialties such as professional turf, landscaping, and horticulture. Less than 1% of CRFs are used in large scale crop production [21-24]. Another challenge is the degradation of currently used coating materials, which are susceptible to either microbes or enzymes. They cannot effectively control the N releases from timely synching to crop uptake over a long period. Some of the coating layers have low degradability that may result in residues left behind in the fields, causing new environmental issues [21, 24]. There is a critical

need to develop an affordable, safe, and effective CRF technology that offers accurately controlled N release; efficient process with low costs; and better biodegradable materials with minimum environmental impacts.

1.3 Research objectives

The goal of this research is to develop an affordable and environmentally friendly control release nitrogenous fertilizer (CRNF) that can control N releasing time and rate to match the timeline of N demand during different stages of corn growth to improve corn yield and nitrogen use efficiency while reducing environmental impact. Three objectives will be completed to achieve the research goals:

1) Activate biochar to improving biochar properties for CRNF development.
2) Develop a biochar-based control release nitrogen fertilizer (BCRNF) by integration of biochar absorption and polylactic acid (PLA) coating
3) Develop an innovative control release nitrogen fertilizer (CRNF) using bio-asphalt mixing method.

1.4 Outline of the thesis

The introduction of the study background is described in Chapter 1. Chapter 2 introduces the experimental study of biochar activation for improving its physicochemical properties. Chapter 3 introduces the work of developing biochar-based controlled release nitrogenous fertilizer (BCRNF) by PLA coating. Chapter 4 introduces the work of developing asphalt-based controlled release nitrogenous fertilizer (ACRNF). Chapter 5 summaries the discovering and conclusions drawn from this study, as well as the recommendations for future CRF research.

CHAPTER 2: EXPERIMENTAL STUDY OF BIOCHAR ACTIVATION FOR IMPROVING ITS PHYSICOCHEMICAL PROPERTIES

2.1 Introduction

Currently, one of the biggest issues of CRF's research is it is extremely difficult to find a suitable N nutrition carrier for CRF. An ideal N nutrition carries should fulfill 2 basic requirements: having an affinity for N-compound (NH_4^+, NO_3^-, etc.), keeping in stable form and state in an agricultural environment. Biochar has the potential to meet these 2 basic requirements, so it was chosen as an N nutrition carrier for CRF in this study.

Biochar (BC) is a carbon-rich material. It is a byproduct generated in biomass torrefaction, pyrolysis, or gasification processes, which is available, renewable, and inexpensive. BC was found to have a strong affinity to inorganic ions (e.g. phosphate, and nitrate, etc.) due to its high specific surface area, numerous polar or nonpolar substances, and porous structure. Moreover, BC can improve soil structure; balance soil acidity; reduce the volatilization of N compounds and enhance water retention when it was applied to soil as a conditioner [25-27]. BC has been proven in a previous study that it is effective to improve N releasing of controlled release fertilizer (CRF) [28]. Chen and his colleague developed a CRF by using BC and waterborne copolymer to coat urea particles [29]. They found that this coating layer was able to control N release and about 65% of N leaching into the water after 22 days of a soil leaching experiment. BC was proven a good nutrition carrier in the BCRNFs [30]. It can effectively adsorb Nitrogen-

phosphorus-potassium (N-P-K) nutrition from solution. When BC combined with N fertilizers (ammonium nitrate, urea), the N use efficiency increased around 12% in corn production [31]. Based on these advantages and previous studies, BC is an ideal ingredient as part of CRFs. However, the adsorption ability of BC, compared with another carbon adsorbent like activated carbon (AC), it's relatively low. Methylene blue (MB) adsorption is an important parameter to reflect the adsorption ability for one material. MB adsorption of BC is only 18.94 mg/g but one commercial AC is 400 mg/g [32]. For BCRNF, BC's adsorption ability is key to delay N-release. To make BC has better adsorption performance as one part of BCRNF, it is necessary to develop one effective method to improve the adsorption ability of BC.

Steam-activation was designed to improve BC adsorption in this study. Based on reaction 1, Under high temperatures, carbon will react with water and then becoming gases. For biochar, a sort of carbon-rich material, it is expected that under high temperature, water can react with some carbon in the surface of biochar to produce more pores. The more porous structure of biochar is promising to have a big improvement in its adsorption ability. Reaction 1: $C + H_2O \xrightarrow{\Delta} CO + H_2$ (1)

Besides activating biochar, nanocellulose is considered to incorporate with BC make biochar has stable form and stronger adsorption ability. Cellulose is a polysaccharide that exists in most plants. It is the most prevalent polymer on earth. Several different physical and chemical processes can be used to produce nanocellulose from cellulose derived from biomass [34]. If upgrading celluloses into nanocelluloses such as cellulose nanocrystal (CNC), cellulose nanofibrils (CNF), their special nanostructure is expected to combine

with powder of BC more tightly which bring the stable form for BC as N carrier nutrition.

The objectives of this study are to 1) explore a method and optimize conditions to improve the adsorption ability of BC. The adsorption of activated BC should approach activated carbon (AC); 2) To form a stable shape of films for future BCRNF applications. To compare their adsorption ability and evaluating the effect of biochar steam activation, MB adsorption of different films will be measured by ultraviolet-visible spectroscopy (UV-vis.). Furthermore, to explore the films' moisture resistance as part of BCRNF, this study will measure the moisture uptake of films in a wet environment. Undergraduate assistant Madison Best conducted this part of the work. The microstructure of the films will be characterized by scanning electron microscope (SEM) to disclose the mechanism of different MB adsorption and moisture adsorption behavior of the films.

2.2 Materials and methods

2.2.1 Materials

The nanocellulose used in this study was purchased from the University of Maine Process Development Center (Orono, Maine). The BC was produced from the pyrolysis of corn stalks in the Bioprocessing Lab at South Dakota State University (Brookings, SD). In this study, all of the solutions were prepared with distilled water. All chemical reagents were in analytical grade.

2.2.2 Biochar Activation

In the BC activation process, the biochar activation reactor was set to operate steam-activation for biochar. This reactor was composed of 2 major systems: steam generator

system and biochar activating furnace system. The steam generator system consisted of a water pump (Series I Pump-110SFN01), a nitrogen cylinder, and a tube furnace (GSL-1100x) as the first heater. Biochar activating furnace system consists of a tube furnace (Thermo Scientific Lindberg/Blue M) as the second heater and a steam trap. To ensure gas tightness, 2 systems were connected in strict. The procedures of operating the reactor to activate biochar are as follows: first, in the biochar activating furnace system, 2.5 g BC was pre-loaded in a tube capsulated by the second heater (setting in a specific temperature:700°C, 800, 900°C). Second, the nitrogen valve was turned on to release nitrogen gas with 900 mL/min flow speed from the nitrogen cylinder for 20 minutes to ensure emptying oxygen in the whole system. Third, the water pump was turned on to pump water with 2.5 mL/min input speed into the tube sharing with nitrogen gas and this tube was encapsulated by the first heater setting the temperature at 350 °C. Under this temperature, water inside the tube was gasified and generated steam importing to biochar activating furnace. Eventually, exhausted gas in this furnace will be blown off by nitrogen gas into the water trap. The whole reaction last 40 minutes. Figure 2.1 presents the schematic configuration of the biochar activation reactor.

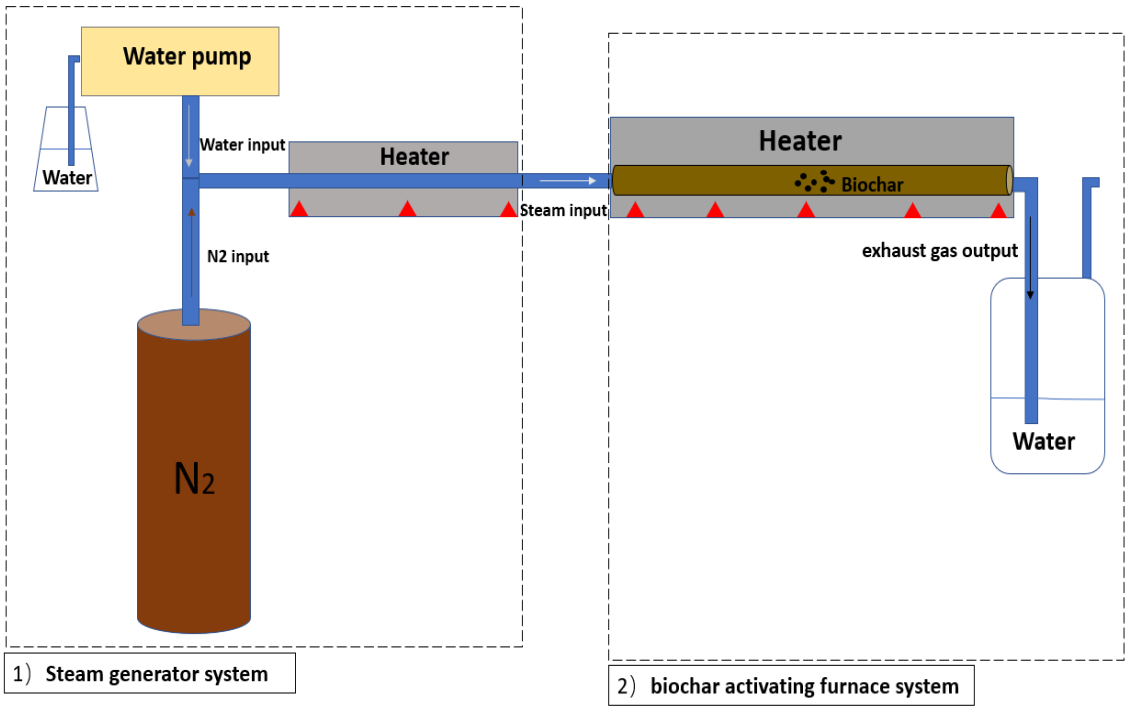

Figure 2.1 Schematic of biochar activation reactor.

2.2.3 Combination of BC, AC, AB, and cellulose nanofibril (CNF)

To combine BC, AC, and AB with CNF, 3% (wt %) CNF solution, the procedures were as follows: first, BC powder was added to a 30 mL beaker along with 15 mL of deionized water. Second, the solution was mixed using a homogenizer (CAT-x120) to create a uniform solution. The probe of the homogenizer was submerged into the solution in the beaker and then mixed the solution for 15 min. Third, after the solution was thoroughly mixed, the solution was poured into a petri dish and placed in a furnace. The samples were dried for 18 hours at 50°C. This was repeated for each percentage of nanocellulose and with each carbon source including BC, commercial AC, and AB. The amount of nanocellulose and nanoparticle were chosen to produce a 0.5 g film with CNF ranging from 5-15%.

2.2.4 Moisture Uptake Testing

To test moisture uptake of BC, AC, and AB films, the procedures were as follows: first, after the film was dried at 105°C for 24 hours, a small sample was taken from the film and then recording its weight. Second, this sample was placed in a pre-setting chamber, fulling with water in the bottom with ~75% relative humidity inside. Last, the mass of a sample was recorded in an interval time. To set up the chamber, the procedures were as follows: first, the lid was placed on top of the chamber, and a plastic hose was attached to one side of the chamber connecting it to a small flask on a hot plate (seen as Figure 2.2). Second, a small flask filled with water was heated 20 minutes to evaporate the water stream flowing into the chamber to raise the relative humidity of the chamber. To ensure keeping this humidity inside the chamber, these procedures were repeated each time when the samples were removed out during measuring mass. Figure 2.2 presents the set up of moisture uptake testing for samples. Water absorption of films was calculated by equation 1:

$$A = \frac{(M_2 - M_1)}{M_2} \times 100 \qquad (2)$$

Where A (g/g) represents water absorption, M_2 (g) is the sample mass after water absorption, and M_1 (g) is the sample mass before water absorption.

Figure 2.2 Moisture Uptake Testing for samples.

2.2.5 MB adsorption experiment

The compared the MB adsorption between different films, the procedures were as follows: firstly, 0.05 g of a film sample was submerged in 50 ml 30 mg/L MB solution under 25 °C. Secondly, after 3 hours, the solution was measured its concentration by UV-vis (UV-2450). Compared to the difference MB concentration in the solution, the MB adsorption quantity can be calculated by equation 2:

$$q = \frac{(C_0 - C)V}{W} \quad (3)$$

where, q (mg/g) is MB adsorption quantity, Co (mg/L) is the original concentration of MB solution, C (mg/L) is the concentration of MB solution after contact with the film 3 hours; V (L) is the volume of solution. W (g) is the mass of film.

2.2.6 Scanning electron microscopy (SEM)

To investigate the surface morphology of BC, AC, AB, and their films. Scanning electron microscopy (SEM) was used to analyze the morphology of films (Hitachi-S-3400, filament-based SEM, MO, USA). Before the SEM test, the samples of films were dried at 60 °C for 48 hours. Subsequently, the samples were coated with gold by the sputter-coater (DC-150, sputtering system, 10 nm of Au). Afterward, the surface of samples were examined under an electric voltage of 10 kV at a working distance of 10 mm with a 1500×magnification.

2.3 Results and discussion

2.3.1 Physical properties of the films

In this study, separately, BC, AC, and AB were successfully combined with CNF as a film form. The diameter of the films are around 70mm. The mass of films are around 500mg. The weight content of CNF in the films are 5%, 10%, 15%. The Ingredient list of different films has been present in table 2.1.

Table 2.1 Ingredient list of different films

Sample	Carbon category	CNF content (wt%)
5-BC	Biochar	5
10-BC	Biochar	10
15-BC	Biochar	15
5-AC	Activated carbon	5
10-AC	Activated carbon	10
15-AC	Activated carbon	15
15-AB-700	700 °C Activated Biochar	15
15-AB-800	800 °C Activated Biochar	15
15-AB-900	900 °C Activated Biochar	15

2.3.2 MB adsorption of different films

Because the 15% CNF films present the best stability, a one-factor analysis was designed for 15% CNF films to evaluate the different MB adsorption of carbon-source films. Table 3 present the MB adsorption quantity of different 15% CNF films. We can see AC films has significantly stronger MB adsorption ability than BC films. For AB films, 15-AB-900 films have 19.58 mg/g MB adsorption quantity, which has approximate MB adsorption with AC films. This result means the activated method for biochar is effective. AB is promising to replace AC as a low-cost carbon source after activation in future research.

Table 2.2 MB adsorption of different carbon source films

Sample	q (mg/g)
15-BC	5.09 ± 1.01
15-AC	19.15 ± 5.71
15-AB-700	14.82 ± 1.54
15-AB-800	14.49 ± 3.43
15-AB-900	19.58 ± 3.01

2.3.3 Moisture uptake test

Figure 2.3 presents the amount of water absorbed by each film sample in an interval time. From figure 2.3, it is shown that for the same kind of carbon-source films, their behavior of water absorption are similar. This indicated that the content of CNF in films does not affect moisture absorption for the films. Besides, AC films present a significantly stronger water absorption than BC films and AB films. This indicates water absorption of AB does not change a lot after steam-activation. Its water absorption ability is still similar to BC. Lower water absorption means AB has better moisture resistance than AC. This

property is useful for future agricultural applications as fertilizer during storage and transportation, preventing the fertilizer are affected by damp.

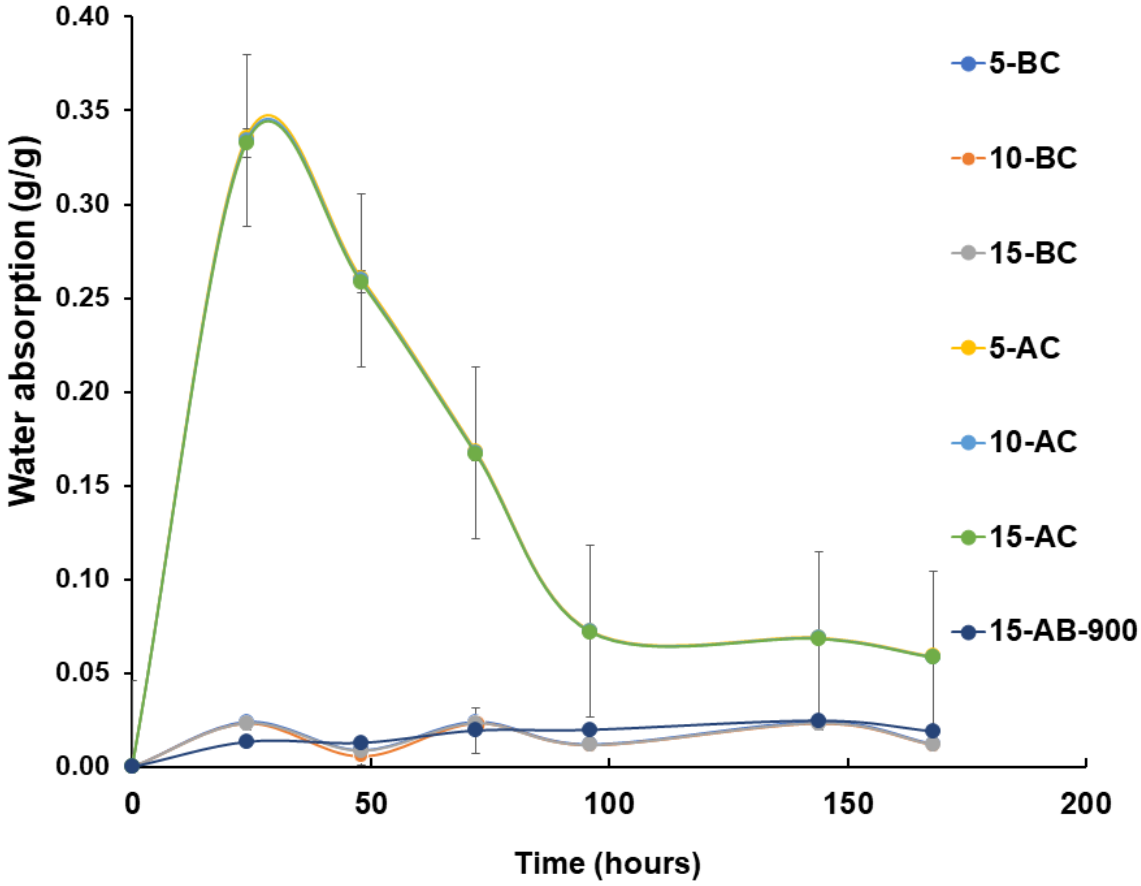

Figure 2.3 Water absorption of different films at different time points.

2.3.4 SEM analysis of different samples

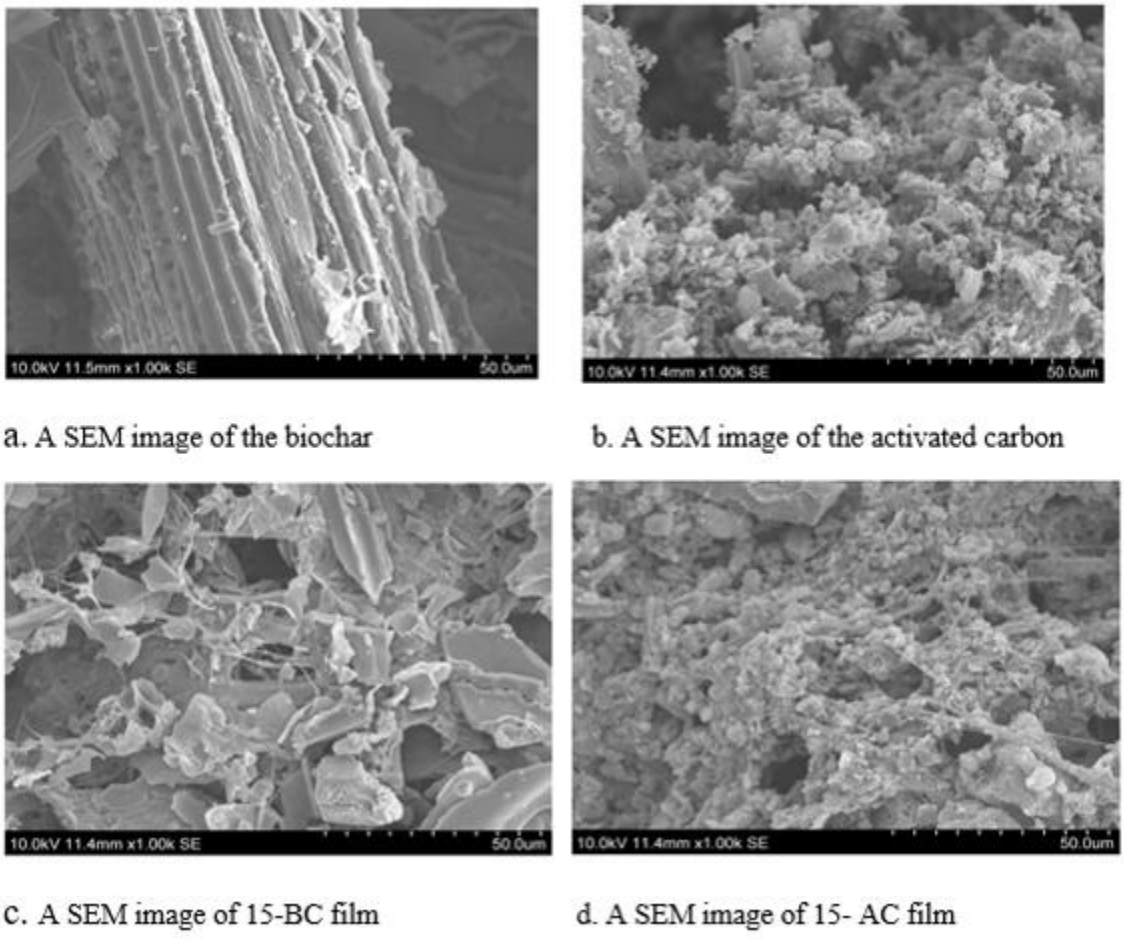

Figure 2.4 SEM of different samples: a) Biochar; b) Activated carbon c)15-BC film; d) 15-AC film.

Based on Figure 2.4, we can see the SEM images showing the structural difference between the biochar and activated carbon. It was observed in Figure 2.4a, 2.4b that activated carbon particles appeared smaller and finer than the biochar particles. Smaller particles and a more porous structure of AC may be a reason that the adsorption ability of AC is stronger than BC. From figure 2.4c and figure 2.4d, we can see CNF has intertwined with biochar, activated carbon in a network structure. That is the reason why 15-AC film and 15-BC film can keep in a stable form. The result of SEM images is

important to reflect the reason 15% of CNF films keep in a stable form. It proves biochar and activated carbon can connect with CNF in a stable connection. This result is meaningful for future research of a combination of carbon materials and nanoparticles.

2.4 Conclusions

From this study, we can see using the steam method to activate biochar to improve its adsorption ability is effective. The AB film is even as good as the AC film in MB adsorption. Therefore, it proves that steam-activation is effective to improve biochar's adsorption ability. This part of the study reaches the objective that improving biochar properties for future controlled release nitrogen fertilizer production. It is worthy to invest more capital and time to optimize steam-activation methods for biochar. On the other hand, the films composed of AB and CNF present a stable shape of a film. It also presents a low moisture uptake in a humid environment. These advantages of AB films indicated the AB-film is promising to apply in controlled release fertilizer. The combination of AB and nano materials are instructive for future carbon material research.

CHAPTER 3: ASSESSMENT OF A BIOCHAR-BASED CONTROLLED RELEASE NITROGEN FERTILIZER COATED WITH POLYLACTIC ACID

3.1 Introduction

There are several challenges needed to be addressed in existing CRFs. First, they are more expensive than conventional N fertilizers because of their complicated production processes and costly coating materials. This limits their applications to high cash crops or specialties (e.g. professional turf, landscaping, and horticulture), with less than 1% being used for large-scale crop (e.g. corn) production [21-23, 35]. Second, many of the coating materials used in the CRFs have been identified non-biodegradable, resulting in new environmental concerns. For example, the coating materials like thermoplastic used in CRFs are very chemically stable to be degraded in soil, in which residues may be cumulated in fields and cause new pollution issues [21, 35]. Third, many of commercial control release fertilizers were claimed capable of continually releasing NH_4^+ up to 30 weeks, but their N release time and rate were unstable since the coating materials like sulfur-coated or bio-based polymers are susceptible to microbial or enzymatic degradation in soils. Many efforts have been made to develop effective and environment-friendly coating materials for CRFs in recent years, but there are very few successful products that can control nitrogen release to match the timeline of N demand for crop like corn growth reported in literature [36]. To address the challenges, there is a critical need to develop an innovative CRF with controllable N release while still remain environmentally friendly properties at relative low-cost.

Biochar may be a good carrier of N nutrients for developing an innovative CRF. As byproduct, biochar can be produced from biomass torrefaction, pyrolysis, or gasification in biofuel production. Since many biomass feedstocks used for biofuel production are assigned to forest wastes and crop residues like corn stover, wheat straw, etc., they are abandoned, inexpensive, renewable, and readily available. Currently, biochar is treated as waste and cost disposal fees in biofuel productions. If this biochar were used for fertilizer fabrication, it not only benefits the biofuel industries, but also can be continually supplied in large quantity at a relative low cost. Moreover, it's proven that biochar has a strong affinity to inorganic ions (e.g. phosphate and nitrate) due to its large surface area, surface functional groups, micro pores and porous structure. Biochar can adsorb nitrogen-phosphorus-potassium (N-P-K) from aqueous solutions, thus, it has been used as nutrition carrier in development of CRFs [30]. In 2020, Puga et al [31] reported a 12% increase in NEU for corn production by mixing biochar with conventional N fertilizers. Also, biochar is found a good soil conditioner [30]. Biochar can increase organic matter and improve soil stabilization and retention of nutrients and water [37-38]. The benefits and outcomes of application are depending on what type, when, and how biochar are applied in soil. The carbonization temperature during biochar formation significantly affect the quality of produced biochar. Generally, proper temperature (e.g. 500 to 600 °C) of biomass carbonization can result in high carbon content and porosity in the produced biochar [39]. Quality biochar can increase carbon sources and energy to support microbial activities and provided a reservoir of organic N, P, K, and other nutrients in soil for plant uptake [40]. It was confirmed that the biochar produced from biomass pyrolysis at about 550 °C have very high carbon content and porosity. There are large amounts of

OH, COOH, C-OH, C-O, C-N functional groups, and O-containing groups distributed on the biochar surfaces, or trapped in micro pores and mesopores. These characteristics make the biochar suitable for directly applying in soil or as nutrient carrier for fertilizer fabrication [30, 37-38]. Nonetheless, the N release of existing biochar-based CRFs was still failing to match the timeline of N demand during corn growing.

Biomass-derived polylactic acid (PLA) was considered a candidate of coating material in this study since it had been identified a biodegradable and hydrophobic biopolymer. When N fertilizers were coated by PLA solution, the N release was controlled by the thickness and surface mophorgy of the coating layers [42-43]. Calcagnile and his colleagues [44] found that PLA-coating was able to decrease the N-release rates approximate 40% in water when compared PLA-coated and uncoated fertilizers. Although PLA is relatively expensive, there is still a possibility to make CRFs economically competitive if properly combing biochar and PLA coating during CRF fabrications. Therefore, PLA was used as coating material and then integrated with biochar to develop an innovative biochar-based controlled-release nitrogen fertilizer (BCRNF) in this study. It was hypothesized that integration of biochar absorption and PLA coating layer would be improving the N releasing time and rate of BCRNF in both water and soil environments. The effects of different PLA concentrations of coating layers on N releasing would be examined. The characterizations of the BCRNFs' physical and thermal properties were also carried out. The ultimate goal is to develop an affordable, environmentally friendly, and effective CRF product that can offer controllable N release to synchronize with the timeline of corn growth.

3.2 Materials and methods

3.2.1 Materials

In order to compare with conventional N fertilizers, ammonium sulfate (21-0-0) were selected as the model of N fertilizer in this study and purchased from local markets. Methylcellulose was acquired from the Candle Makers Store in U.S. Sandy soil was purchased from the local Lows Store. PLA was purchased from the Solutions of Consequences LLC (Grand Rapids, Michigan). In this study, all of the solutions were prepared with distilled water. All chemical reagents were of analytical grade.

3.2.2 Preparation of Biochar

The biochar used in this study was produced from pyrolysis of corn stover in the Bioprocessing Lab at South Dakota State University (SDSU), Brookings, SD 57007. To prepare the biochar, corn stovers was collected from the corn field of experiment station farm at SDSU. The corn stover was air-dried to moisture content less than 12% and then grounded into powder with 90% of particles' diameters less than 1 mm. After that, the powder was pyrolyzied into three products (syngas, bio-oil, and biochar) in a reactor (capacity of 3 kg per hour) at about 550 °C. During pyrolysis process, many reactions (e.g. dehydration, fragmentation/depolymization, carbonazation, repolymization, oxidation, etc.) were taking place to break down the long-chain large molecules of lignin, celluloses, and hemicelluloses of corn stover into short-chain smaller molecules of liquid bio-oil (mainly containing aromatics and other hydrocarbons, phenols, organic acids, water, etc.), syngas (a gas mixture of CO_2, H_2, CO, CH_4, steam, etc.), and solid biochar (contained over 70% of carbon with rest of minerals and ash). The properties, compositions, and yield proportions of these three products are heavily affected by

feedstock species, reactor type, and operating conditions. The syngas and bio-oil are used to produce biofuel products, but the biochar is currently treated as waste in biofuel industries. More details of pyrolysis of corn stover were described in our previous work [52]. The biochar used in this study had been stored in plastic bags over two years. The bulk density of this biochar was 0.095g/cm^3 with 3.44% of moisture content before being used to fabricate the BCRNF samples. The fresh biochar produced by biomass pyrolysis may contain traces of various organics (e.g., aromatic hydrocarbons, phenols, organic acids, and other hydrocarbons, etc.) on its surface, which may cause negative effects in soil amendment [52]. If biochar was aged or stored for a certain time, those organics may be volatilized from biochar or degraded into unharmful compounds. The biochar used in this study had been stored in plastic bags over two years. The bulk density of this biochar was 0.095g/cm3 with 3.44% of moisture content before being used to fabricate the BCRNF samples.

3.2.3 Preparation of biochar-based nitrogen fertilizers (BNF)

In our preliminary experiment, the maximum adsorption capacity of biochar for ammonium sulfate was a mass ratio of 1:5 (biochar to ammonium sulfate) without or very little of the ammonium sulfate crystal particles appeared in the mixture. To make sure ammonium sulfate was completely impregnated or absorbed into the micropores of biochar for controlling N release. A mass ratio of 1:1 (biochar to ammonium sulfate) was chosen to prepare the BNF samples in this study. To prepare BNF, 150 g of ammonium sulfate was dissolved in 200 ml of deionized water and stirred at room temperature (25 °C) for 20 minutes. After that, 150 g of biochar was slowly loaded to the ammonium sulfate solution and continually stirred for 20 minutes to remove the air and porous

spaces inside the powder using a 2000 mL beaker, followed by adding 15.8 g of kaolin clay into the uniform mixture of biochar and ammonium sulfate with an extra stirring for 20 minutes. Then, the mixture was dried to impregnate ammonium sulfate into the micropore and mesopore or on surfaces of biochar in an oven at 65 °C for 5 hours. After mixing and drying, the volume of biochar as well as the volume of the mixture were significantly reduced to less than 500 ml. Afterward, the dried mixture was blended with 16.62 g methylcellulose and 10 mL deionized water and then pelletized into particles with 3 mm in diameters and less than 5 mm in length using a small pelletizer (Nesco FG-180). The sample of these particles was named biochar-based nitrogen fertilizers (BNF).

3.2.4 Preparation of biochar-based control released fertilizer (BCRNF)

To prepare BCRNF samples, PLA pellets were dissolved in 99% of chloroform solvent to individually prepare three different solutions with 3%, 6%, 10% of PLA in weight. The BNF particles prepared earlier was submerged in each PLA solution to coat the surface of BNF particles. After all particles were fully coated with the PLA solutions, they were taken out and separately lay out on different plates. All coated BCRNF samples were air-dried at room temperature (20 ± 2 °C) for 8 hours to remove the residues of chloroform solvent to get the final samples of BCRNFs. Based on the coating concentration of PLA solution, these three different BCRNFs were named BCRNF-P3, BCRNF-P6, and BCRNF-P10, respectively. The raw biochar powder, conventional ammonium sulfate fertilizers, and the produced BCRNF particles were shown as Figure 3.1. The differences in appearances of BCRNF-P3, BCRNF-P6, and BCRNF-P10 particles could not be distinguished by naked eyes. Our preliminary estimations showed that less than 5% of change in the weights of fertilizer particles before and after PLA

coating. Generally, the higher concentration of PLA solution was used, the thicker coating layer would be acquired, which resulted in less than 1% of weight difference in average between BCRNF-P3, BCRNF-P6, and BCRNF-P10 particles.

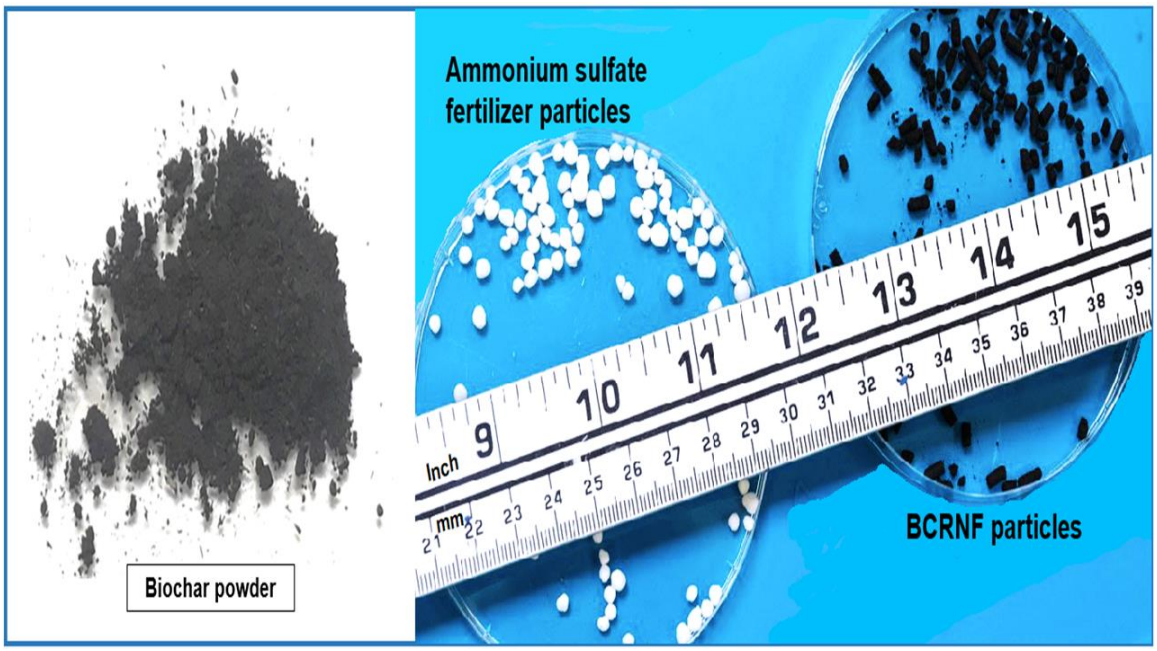

Figure 3.1 The biochar and conventional ammonium sulfate fertilizer used to prepare BCRNF particles

3.2.5 Experimental design of N-release in water

Referred to the previous studies [46-47], the experiment of N release of BCRNF in water was carried out by following these three steps: Firstly, 1 g of each sample of BCRNF-P3, BCRNF-P6, and BCRNF-P10 was individually submerged into 100 mL deionized water inside an air tight bottle. Meanwhile, the same amount of conventional ammonium sulfate and BNF were also tested respectively as control. Second, the NH_4^+ concentration of each sample solution inside the bottle was measured and recorded daily by using an ammonium Ion Specific (ISE) meter (Oakton) until the NH_4^+ concentration

had no change for at least 48 hours. Each measurement was performed in triplicate. The measured NH_4^+ concentration was used to represent N release of each sample in this study. The cumulative N release (%) of each sample was calculated with equation 3:

$$N_i = \frac{C_i * V_i}{N_c * m_t} * 100\% \quad (4)$$

Where, N_i is the cumulative N release (%) in the water on the i_{th} day. C_i (g/L) is the NH_4^+ concentration of the solution on the i_{th} day. V_i (L) is the water volume, m_t (g) is the total mass of BCRNF sample submerged in the water. N_c (%) is the percentage of NH_4^+ in the initial BCRNF sample before submerged in the water.

3.2.6 Experimental design of N release in soil

An experiment of soil columns was designed to investigate the N release of BCRNFs in sand soil under a simulation of natural rainy environment. The experiment was carried out by simulating the N release of BCRNF in sand soil under both storm and regular raining conditions. PVC transparent columns with 7.5 cm in diameter and 25.5 cm in height were used to run this experiment. Figure 3.2 shows a schematic diagram of the soil column design for the N leaching in the soil column experiment. The experiment was performed by following this procedure: First, to reduce the loss of soil during the experiment, a filter paper was put at the bottom of the column before loading soil and samples. Second, a total of 1738 g of sand soil was loaded into each column. The height of sand soil in the column was about 23.3 cm. Third, 3 g of each sample were buried in the soil at a depth of 5 cm. To simulate natural raining environment, the parameters of watering were selected from the model established by Goodrich et al [48]. Second, by simulating a storm, 7000 ml of deionized water was continuously fed into the inlet on top of the column at a flow rate of 20 ml/minute and flushed the soil throughout the column

using a liquid peristaltic pump (GP 1000, Fisher Scientific). The effluent leachate from the column outlet was collected in a glass jar. Third, the NH_4^+ concentration of the leachate from each sample was measured and recorded using the ammonium Ion Specific (ISE) meter. After that, the soil column was flushed with 1000 mL of deionized water at the same flow rate by the pump every three days to simulate regular raining conditions until the NH_4^+ concentration in the leachate had no change. The leachates generated from the new water flushing were separately collected in new bottles. The purpose of the periodic flushing was to stimulate regular rain-washing-soil in real environment [49]. The same amount of conventional ammonium sulfate and BNF were also tested as control. Each test was performed in triplicate. Again, the NH_4^+ concentration of leachate was used to represent the N release (%) of the samples in the sand soil, which were calculated with equation 4:

$$N_i' = \sum_{i=0} \frac{C_i' V_i'}{N_c * m_t} \quad (5)$$

Where N_i' is the total cumulative NH_4^+ release (%) in the leachate on the i_{th} day. C_i' (g/L) is the NH_4^+ concentration of the leachate on the i_{th} day. V_i' (L) is the volume of the leachate on the i_{th} day. m_t (g) is the total mass of the BCRNF sample applied into the column, and N_c (%) is the percentage of NH_4^+ in the initial BCRNF sample before applying in the columns.

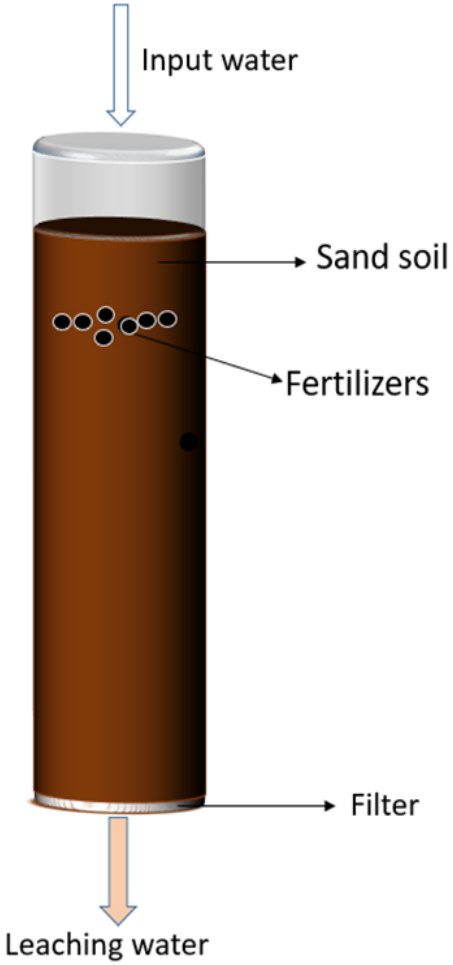

Figure 3.2 Schematic of a soil column for N leaching experiment.

3.2.7 Water absorbance and retention of BCRNFs

Water absorbance of BCRNFs was investigated by following the steps established in previous research [30]. 0.5 g of each sample (BNF, 3%, 6%, and 10% BCRNFs) was dried in an oven under 60 °C for 48 hours. Afterward, the dried samples were conditioned in an air tight chamber with constant 75% relative humidity (RH). The weight change of each sample was measured and recorded daily during the conditioning until the sample weight became stabilized. Water absorbance was calculated with equation 5:

$$W_A = \frac{(M_2 - M_1)}{M_1} \times 100\% \quad (6)$$

Where, W_A (%) represents water absorbance, M_2 (g) is the sample weight after water absorption, and M_1 (g) is the sample weight before water absorption.

The water retention of BCRNF was investigated by following the steps established in previous research [30]. After the water absorption tests were finished, the relative humidity inside the chamber was conditioned to around 50%. The sample weights of BCRNFs were measured and recorded in an interval of 24 hours until the sample weights had no changed. The water retention is presented by the rate of water lost over time. The lower water lost, the higher water retention. The water loss was calculated with equation 6:

$$W_l = \frac{(W_1 - W_2)}{W_1} \times 100\% \quad (7)$$

Where, W_l (%) is the water loss of a sample to represent its water retention. W_1 (g) represents the weight of the sample before losing water. W_2 (g) represents the weight of the sample after losing water. As control, the water absorbance and retention of BNF were also tested in this study. Each test was performed in triplicate.

3.2.8 Scanning electron microscopy (SEM) analysis

The microstructures of BCRNFs coated with different concentrations of PLA (3%, 6%, and10%) were examined using a SEM (Hitachi-S-3400, filament-based SEM, MO, USA). Before SEM observation, the BCRNF samples were first dried at 60 °C for 48 hours. To evaluate the surface microstructure of BCRNFs, the samples were then dipped into liquid nitrogen and fixed on the support. Then, they were coated with Au using a sputter-coater (DC-150, sputtering system, 10 nm of Au). Ultimately, the surfaces of BCRNF particles were observed and pictured under an electric voltage of 10 kV at a working distance of 10 mm with a 1500 × magnification.

3.2.9 Thermal stability analysis

To investigate the thermal stability of BCRNFs, the BCRNF samples were analyzed using a Thermogravimetric analyzer (TGA) (Q5000SA, TA instruments, USA). Referred to the standard operational procedure of TGA analyzer, the TGA analysis was carried out as following steps: firstly, 3 mg of each sample of BNF, BCRNF-P3, BCRNF-P6, and BCRNF-P10 were individually put into different aluminum pans. Then, the pans loaded with samples were put in the furnace of TGA and then heated up from 20 to 450°C under a nitrogen atmosphere at a heating rate of 10 °C /min with a gas flow rate of 20 mL/minute. An empty aluminum pan was also tested as a reference.

3.2.10 Statistical analysis of experimental results

All the values of final results shown in the figures and tables are the means of three replications. The data was subjected to one-way ANOVA to identify the significances between different treatments at 95% of confidence level.

3.3 Results

3.3.1 N-release of BCRNFs in water

The cumulative N-releases of different BCRNFs and the BNF and conventional ammonium sulfate fertilizers in water are shown as Figure 3.3. The ammonium sulfate and BNF show exponential N releasing patterns. Up to 90% N of ammonium sulfate and 76% N of BNF were released into water within day 1. After day 1, the concentration of NH_4^+ in their water solutions were no longer changed, which means no more N releasing from the samples of ammonium sulfate and BNF. In contrast, only 1.82% N of BCRNF-P10, 3.22% N of BCRNF-P6, and 10.58% N of BCRNF-P3 released into water in day 1.

For the BCRNF samples, the BCRNF-P3 also shows an exponential N release in day 2 and 3. After its 74% N released in day 3, there was no more N releasing from BCRNF-P3, and the concentration of NH_4^+ was stable. However, the N release of BCRNF-P10 and BCRNF-P6 were continually releasing in linear pattern at a lower releasing rate until day 12, and then went to stable at the level of about 70% N release. Figure 3.3 also shows that there was no significant difference in N release between BCRNF-P6 and BCRNF-P10, but the N release of these two samples were significant difference from that of other 3 samples: ammonium sulfate, BNF, and BCRNF-P3. The measured results of BCRNF-P10 had very low standard deviation. This indicates that the measurements were very stable with high repeatability. Therefore, the error bars on the N release curve of 10 % PLA BCRNF is hard to be seen in Figure 3.3.

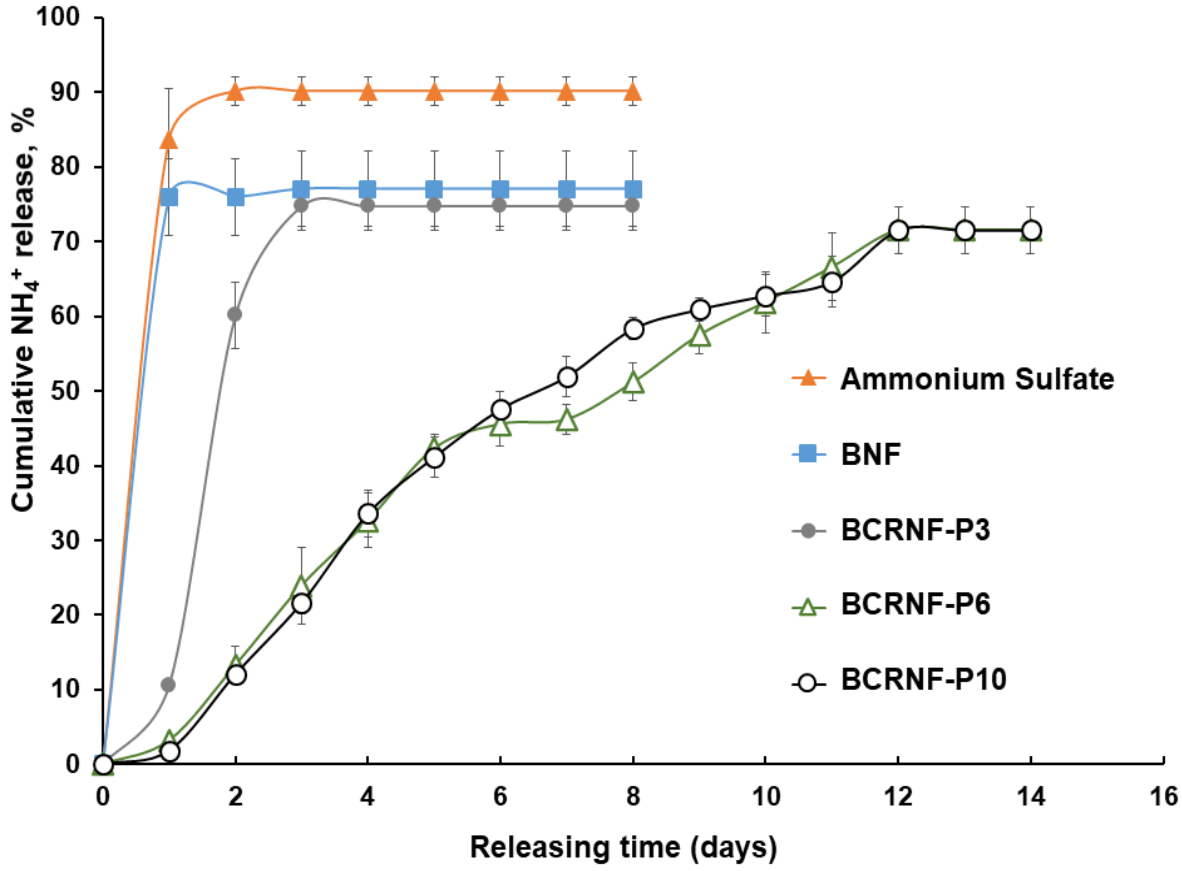

Figure 3.3 The cumulative N-release of different BCRNFs and control fertilizers in water. Ammonium sulfate is the conventional N fertilizer; BNF is biochar-based nitrogen fertilizer; BCRNF-P3 is the BCRNF coated with 3% of PLA solution; BCRNF-P6 is the BCRNF coated with 6% of PLA solution; and BCRNF-P10 is the BCRNF coated with 10% of PLA solution.

3.3.2 N-release of BCRNFs in soil

The N releases of different BCRNFs and the BNF and conventional ammonium sulfate fertilizers into leachates in the soil column experiment under simulating conditions of rain-washing-soil are shown as Figure 3.4. On day 1, the test was performed under simulating conditions of storm rain-washing-soil. After a total of 7000

ml water continually flushed through the soil column at a flow rate of 20 ml/minute for 6 hours, 57 % N of ammonium sulfate and 56% N of BNF were washed out into the leachates on day 1. In contrast, about 53% N of BCRNF-P3, 15% N of BCRNF-P6, and 6 % N of BCRNF-P10 were released into the leachates. However, started from the day 3 or later, the soil columns were flushed with 1000 ml water to simulate regular rain-washing-soil. There was very little N release detected in the leachates for the columns of ammonium sulfate, BNF, and BCRNF-P3. It was observed that there were still about 15% N of BCRNF-P6 and 20 % N of BCRNF-P10 released into the leachates under the same conditions on the day 3. As the simulation of regular rain-washing-soil ongoing, there were less and less N-release into the leachates and no N release after 25 days. The BCRNF-P10 showed the longest N-releasing time (25 days), followed by BCRNF-P6 (19 days), BCRNF-P3 (4 days), BNF (1 day), and ammonium sulfate (1 day). Similarly, the measured results of BCRNF-P10 had very low standard deviation. This indicates the results were very stable with high repeatability. Therefore, the error bars on the N release curve of BCRNF-P10 is hard to be seen in Figure 3.4. The N release patterns of all samples in the experiment of soil column seemed matching well with their patterns of N release in water (Figure 3.3).

In summary, the total cumulative N release of each sample into leachate during the soil column experiment are shown as Figure 3.5. Compared to the total of 59% N of ammonium sulfate, 58% N of BNF, and 56% N of BCRNF-P3 were leaching out the soil columns, the BCRNF-P10 had the least 34% N released into leachate, followed by the BCRNF-P6 lost 40% N. These results indicate that after a simulation of the raining season, 66% N of BCRNF-P10 and 60% N of BCRNF-P6 remained in the soil available

for crop uptake, but ammonium sulfate, BNF, and 3% PLA BCRNF just remained 41%, 42%, and 44% N in soil, respectively. These results indicate that it is very difficult to have NUE more than 40% if directly applied ammonium sulfate in soil for crop production.

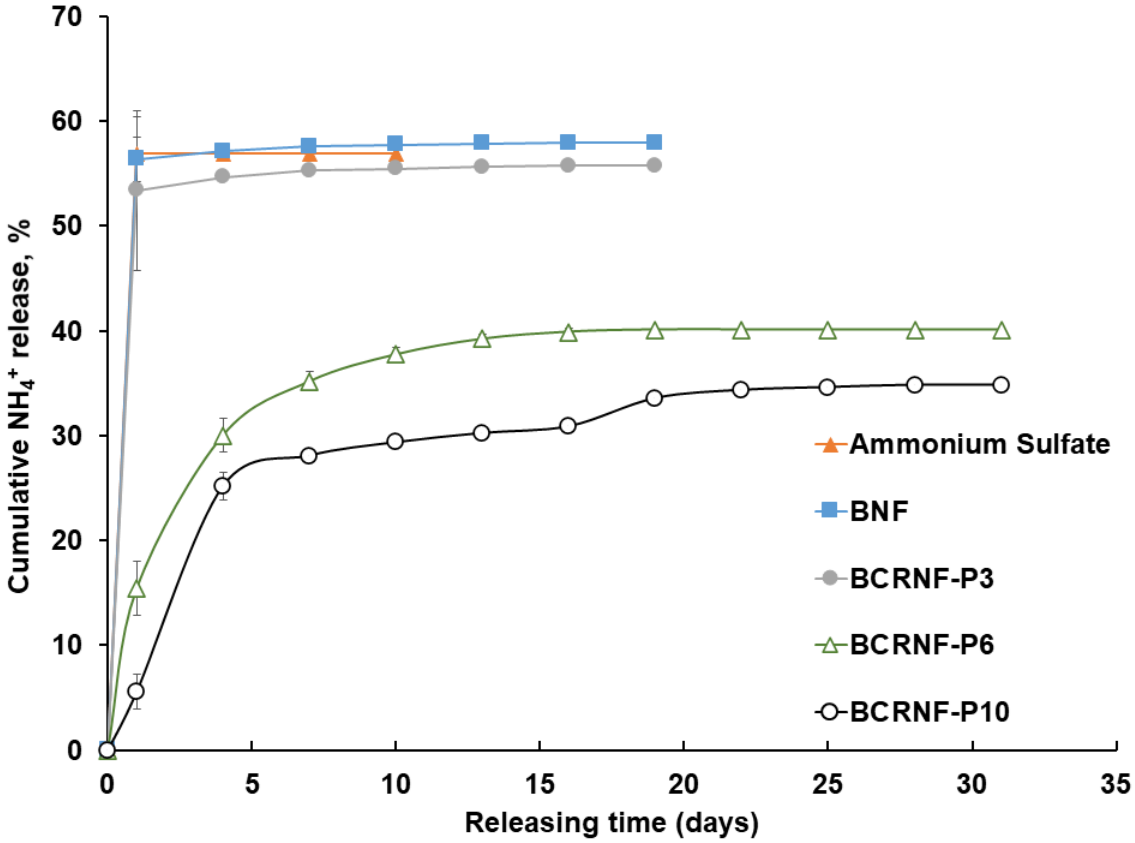

Figure 3.4 The cumulative N-release of different BCRNFs and control fertilizers in leachates in the experiment of soil columns. Ammonium sulfate is the conventional N fertilizer; BNF is biochar-based nitrogen fertilizer; BCRNF-P3 is the BCRNF coated with 3% of PLA solution; BCRNF-P6 is the BCRNF coated with 6% of PLA solution; and BCRNF-P10 is the BCRNF coated with 10% of PLA solution.

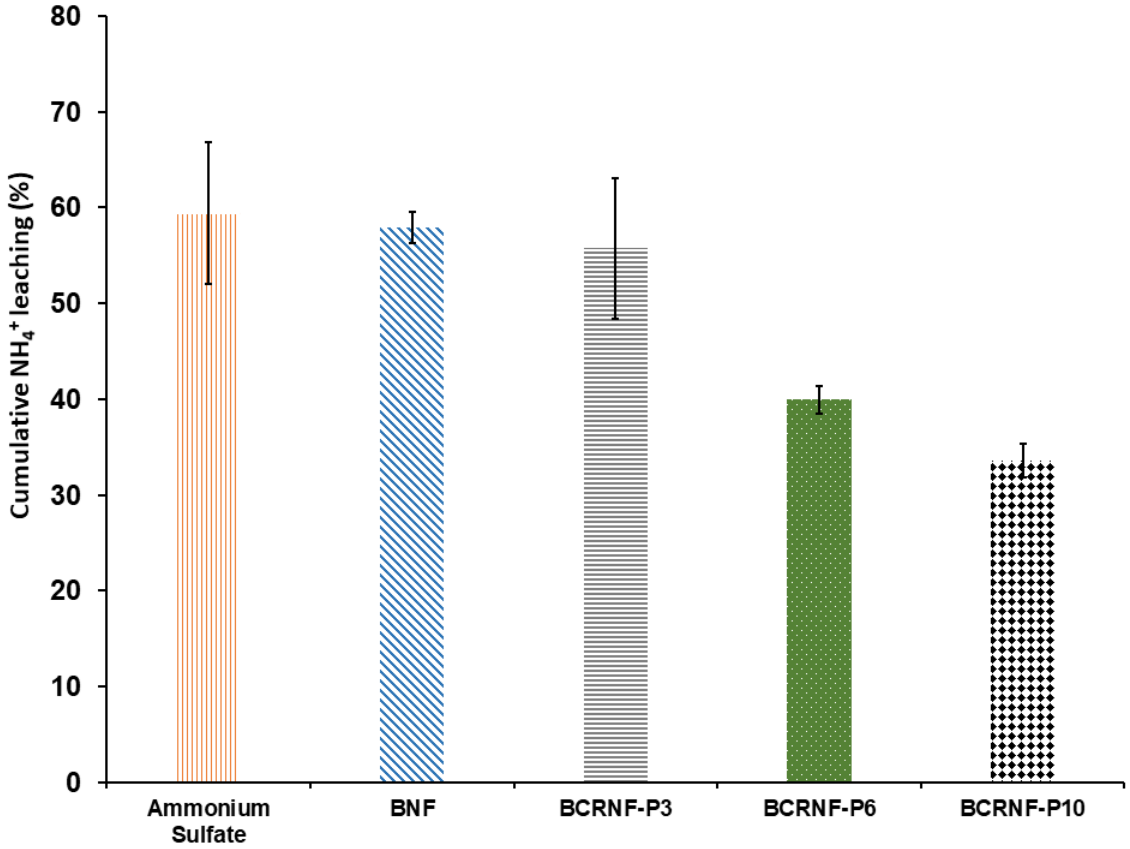

Figure 3.5 The total N-release of different BCRNFs and control fertilizers in leachates in the experiment of soil columns. Here, ammonium sulfate is the conventional N fertilizer; BNF is biochar-based nitrogen fertilizer; BCRNF-P3 is the BCRNF coated with 3% of PLA solution; BCRNF-P6 is the BCRNF coated with 6% of PLA solution; and BCRNF-P10 is the BCRNF coated with 10% of PLA solution.

3.3.3 Water absorbance and retention of BCRNFs

The water absorbance of different BCRNFs and BNF are shown as Figure 3.6. All fertilizer samples showed the maximum water absorbances in the first day by following this order: BNF > BCRNF-P3> BCRNF-P6 > BCRNF-P10. The absorbances of all samples decreased over time after day 1. It was observed that there was significant change in water absorbance between BCRNF-P10 and all other samples after the 6^{th} day.

BCRNF-P10 had significant higher water absorbances than that of other samples after 6 days. The BCRNF-P10 showed the highest water absorbance among the samples in the period from the 7^{th} to 10^{th} day. After 10 days, BNF reached the saturated water absorption of equilibrium state at the earliest time among the samples, followed by BCRNF-P3 (13 days), BCRNF-P6 (14 days), and BCRNF-P10 (15 days).

The water loss (%) of sample was used to represent its water retention capacity in this study. The water loss of different BCRNFs and BNF are shown as Figure 3.7. Started from the saturated state of water absorption, the water loss (%) of all samples decreased sharply in the first day by following this order: BNF > BCRNF-P3> BCRNF-P6 > BCRNF-P10. It was observed that BCRNF-P10 had significant lower water loss than that of all other samples until the day 3. After that, BCRNF-P6 and BCRNF-P3 had lower water loss than that of BNF and BCRNF-P10 until reached a new lowest saturated water equilibrium on day 4. The BCRNF-P10 continually lost water until reached the lowest water equilibrium state on day 5. It was found that all BCRNFs and BNF samples can retain water for 4 days or more. Especially, BCRNF-P10 can retain water in the longest time (5 days).

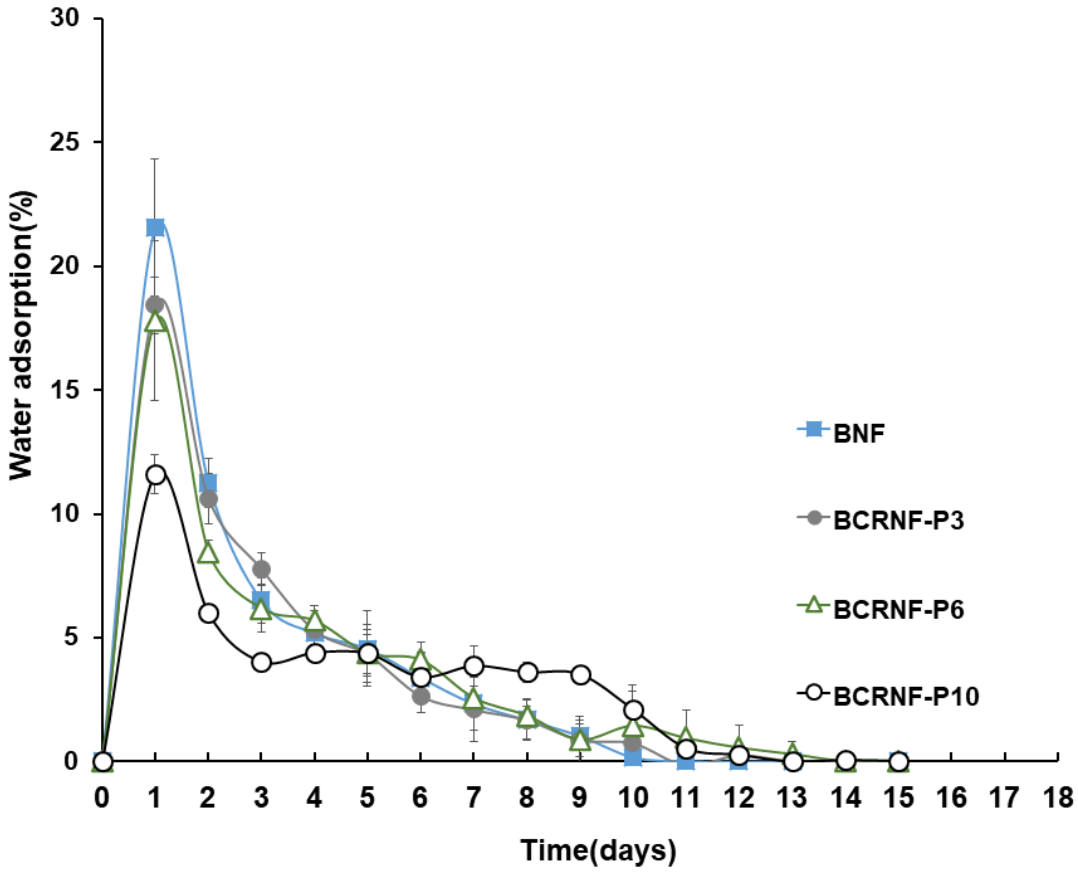

Figure 3.6 Water absorbance of different BCRNFs and BNF. Here, BNF is biochar-based nitrogen fertilizer; BCRNF-P3 is the BCRNF coated with 3% of PLA solution; BCRNF-P6 is the BCRNF coated with 6% of PLA solution; and BCRNF-P10 is the BCRNF coated with 10% of PLA solution.

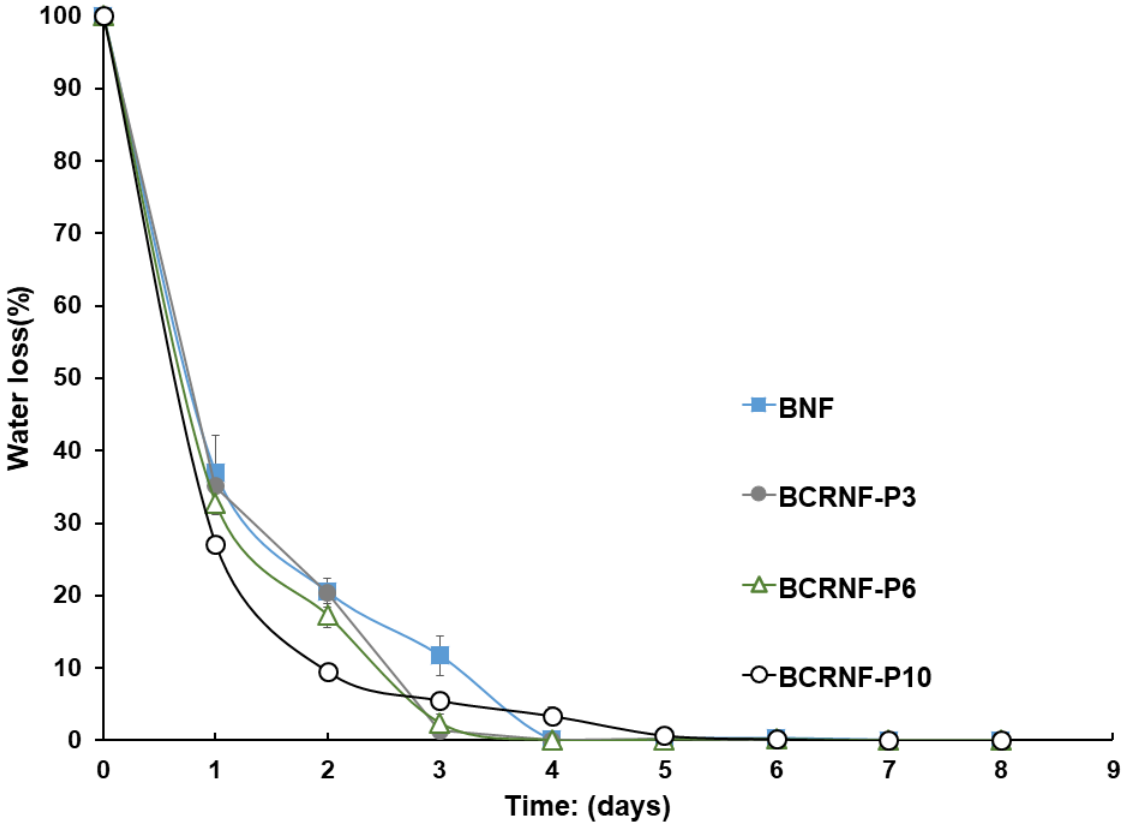

Figure 3.7 Water loss of different BCRNFs and BNF. Here, BNF is biochar-based nitrogen fertilizer; BCRNF-P3 is the BCRNF coated with 3% of PLA solution; BCRNF-P6 is the BCRNF coated with 6% of PLA solution; and BCRNF-P10 is the BCRNF coated with 10% of PLA solution.

3.3.4 Surface morphology of BCRNFs

The SEM images of BCRNFs and raw biochar are shown to compare their microstructure and surface morphology in Figure 3.8. The image of Figure 3.8a shows the initial porous structure and rugged morphology on the surface of raw biochar before being used to fabricate BCRNF samples. Respectively, the Figure 3.8b, 3.8c, and 3.8d show the microstructure and surface morphologies of BCRNF-P3, BCRNF-P6, and BCRNF-P10 after coated by different concentrations (3%, 6%, and 10%) of PLA

solutions. When the coating PLA concentration changed from 3%, 6% and 10%, the porous structure and surfaces of biochar particles of the BCRNFs were covered by PLA coating layers, but the surface morphologies were very different from each other. The surface of BCRNF-P3 (Figure 3.8b) was rough with more small pores and cracks. There were much less rough and less small pores and cracks on the surface of BCRNF-P6 (Figure 3.8c). The surface of BCRNF-P10 (Figure 3.8d) became smoother with very few small pores.

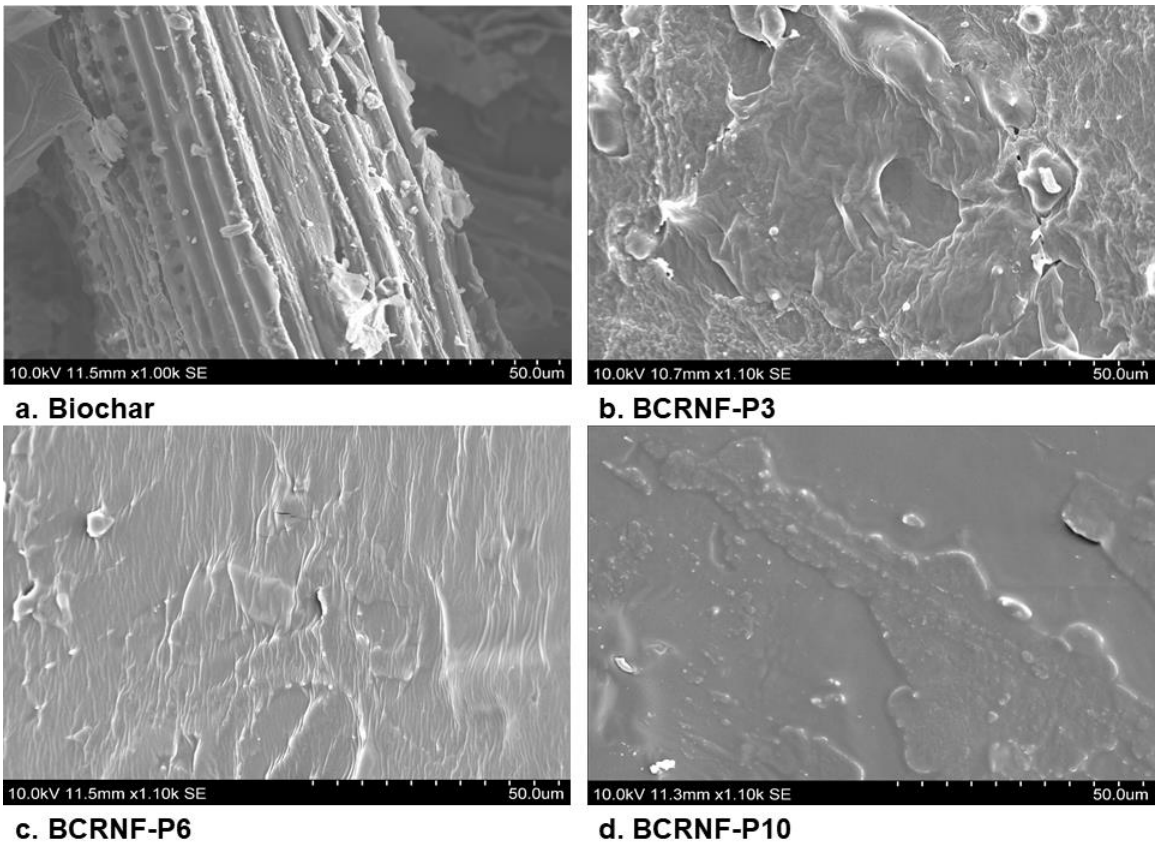

Figure 3.8 The SEM images of different BCRNFs and biochar: (a) raw biochar. (b) BCRNF-P3. (c) BCRNF-P6. (d) BCRNF-P10. Here, BCRNF-P3 is the BCRNF coated with 3% of PLA solution; BCRNF-P6 is the BCRNF coated with 6% of PLA solution; and BCRNF-P10 is the BCRNF coated with 10% of PLA solution.

3.3.5 Thermal stability of BCRNFs

The results of TGA analyses on BCRNFs and BNF samples are shown in Figure 3.9. The plots show the percent mass of different BCRNFs and BNF as functions of temperatures under nitrogen environment. When the samples of BNF, 3%, 6%, and BCRNF-P10s were individually loaded into the TGA analyzer and then heated up from 20 °C to 450 °C, there was no any thermal degradation for all samples until 160 °C, but BNF started to be degraded slowly at about 170 °C due to water evaporation and volatiles released, and then dramatically lost mass from 250 °C to 340 °C because of evaporation of ammonium sulfate starting at 250 °C and ending at 340 °C. After that, the mass loss slowed down a little bit and then completely decomposited at 420 °C without any residue due to biochar completely decompostion. In contrast, the thermal degradation of BCRNF-P3, BCRNF-P6, and BCRNF-P10 began at 230 °C. The degradation rates of BCRNFs were depending on PLA concentration in the range between 230 °C to 380 °C. The order of degradation rates is BCRNF-P3 > BCRNF-P6 > BCRNF-P10. However, the BCRNF-P10 quickly lost mass and stopped degradation with about 18% of mass residue at 380 °C. After 380 °C, if ignored possible measuring errors, the order of degradation rates was reverted, becoming BCRNF-P3 < BCRNF-P6 < BCRNF-P10 between 380 °C to 450 °C. Obviously, there were two stages of thermal degradations for these BCRNFs and BNF samples in the range of 20 °C to 450 °C. In the stage 1, the temperature ranged between 20 °C to 160 °C, with no obvious mass change in all BCRNFs and BNF. For the second stage of temperature ranging from 160 °C to 450 °C, all BCRNF samples were degraded by thermal decomposition and lost more than 80% of their mass. But the thermal

decomposition of BNF was significant different from the 3 samples of BCRNF and even completely decomposed without any residue at about 420 °C.

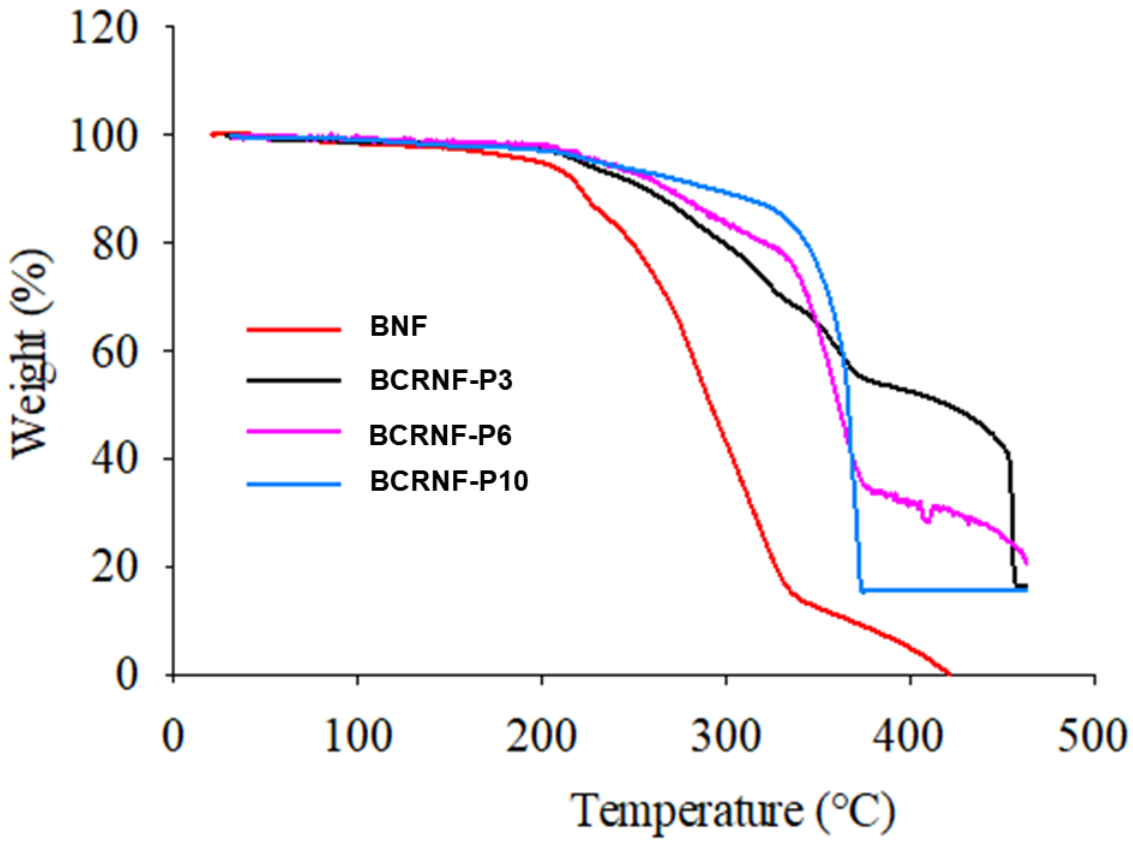

Figure 3.9 The thermal degradation curves of different BCRNFs and BNF in the TGA analyses. Here, BNF is biochar-based nitrogen fertilizer; BCRNF-P3 is the BCRNF coated with 3% of PLA solution; BCRNF-P6 the BCRNF coated with 6% of PLA solution; and BCRNF-P10 is the BCRNF coated with 10% of PLA solution.

3.4 Discussion

3.4.1. Effects of PLA concentrations of coating layers on the N release of BCRNFs

The Figure 3.3 shows that there was no change in the NH_4^+ concentration after 90% N released from the sample of ammonium sulfate into water. This might be because either

the rest of 10% N was held inside the sample or the ammonium sulfate purchased from local market contained only 90% of solvable N (NH_4^+). There was no residue observed in the ammonium sulfate solution after completely discover in water. If ignored the measuring errors or NH_3 evaporation during the experiment, it is reasonable to assume that this ammonium sulfate sample contained about 90% of solvable N. Although there was no significant difference in the total of cumulative N release between BNF and BCRNF-P3, Figure 3.3 identified that the BCRNF-P3 had a longer releasing time at a lower releasing rate to release up to its 74% N into water, which was slightly lower than that of the BNF (released about 76% N). This result indicates that 3% PLA coating layer was able to delay 74%N release for 3 days while the 76% N of BNF released within 1 day. Moreover, the BCRNF-P6 and BCRNF-P10 had 12 days of 70%N releasing time, which was much longer than that of ammonium sulfate, BNF, and BCRNF-P3 in this study. Compared to the N release time of existing CRFs developed by other researchers, for example, 3 days for Ye et al [50], 8 days for Gwenzi et al [30], and 10 days for Li et al [46], the BCRNF-P6 and BCRNF-P10 have achieved a significant improvement. Although the higher (6% and 10%) PLA concentrations resulted in longer releasing time at lower N release rates, it is not necessary to increase PLA concentration over 6% since there was no significant difference in N release between BCRNF-P6 and BCRNF-P10. The lower PLA concentration means the lower mass ratio of fertilizer to coating layer and less cost in the BCRNF fabrication, which will improve the economic survivability of BCRNF products.

Another discovering shown in Figure 3.3 is that biochar can hold about 14% N of BNF particles without PLA coating, not releasing into water. If the BNF particles were

covered by PLA coating layers, more N would be retained inside the particles. When the PLA concentrations of coating layers increased from 3%, to 6% and 10 %, over 16% and 20% of N were retained inside the particles of BCRNF-P3, BCRNF-P6 and BCRNF-P10, respectively. When these BCRNFs were applied in field, one could logically expected that at least 14% N and biochar might remain in soil even after PLA coating layers were completely degraded. Due to the integration of biochar absorption and PLA coating layers, the remained N and biochar not only increase carbon sequestration and energy for microbe activities in soil, but also moderate soil degradation and N leaching into underground water. The results (Figure 3.4) of soil column experiment also demonstrated that the PLA concentrations of coating layers had significant effects on the N releasing time and rate of BCRNFs in soil environment. The higher PLA concentration of coating layer, the longer N releasing time (25 days) of BCRNF-P10 had, followed by BCRNF-P6 (19 days), BCRNF-P3 (4 days), BNF (1 day), and ammonium sulfate (1 day). These results verified our hypothesis: integration of biochar absorption and PLA coating layer would be improving the N releasing time and rate of BCRNF in both water and soil environments.

The controllable N release mechanism of BCRNF is shown as Figure 3.10. When biochar mixed with the dissolving ammonium sulfate, NH_4^+ ions were attached on surfaces and trapped within mesopores and micropores of biochar due to chemisorption of polar and nonpolar compounds, including hydrophobic bonding, π-π electron donor-acceptor interactions resulting from fused aromatic carbon structures, and weak unconventional H-bonds. After the solution was dried into powder, the biochar particles were impregnated with NH_4^+, which are binding through ligand exchange, dissolved

multidentate ligand, C-π-cation interaction, acid-base reactions with COOH, C-OH, C-O, and C-N functional groups on the biochar surface, coordination of deprotonated OH or COOH functional groups, and reactions of O-containing groups [51], shown as Figure 3.10a. The powder of biochar impregnated with $NH_4^+$was pelletized to small particles and then coated with PLA layers to form granular BCRNF particles. When a BCRNF particle starts to absorb moisture and penetrate through the coating layer into the BCRNF core due to swelling and cracking of the coating layer, osmotic pressure builds up and irrigation water penetrates into the surfaces and within mesopores and micropores of biochar to dissolve the impregnated solid N fertilizer to release NH_4^+, shown as Figure 3.10b. Most irrigation water is absorbed by biochar and part of the NH_4^+solution is stored inside the pores of biochar. Then, the dissolved NH_4^+ ions are released to the interface between biochar and coating layer via diffusion, under concentration or pressure gradient, or a combination of these as the driving force. When more water absorbed into the BCRNF core, the stored NH_4^+ solution and water can diffuse to the interface following the dehydration of biochar (Figure 3.10b). With changes in the osmotic pressures of both interfaces of biochar and coating layer and the coating layer and water or soil, the processes of absorption, swelling, diffusion, and dehydration of biochar and coating PLA take place in parallel and series if water shortage occurs in the surrounding soil [29,46-47]. In these processes, the coating layer works as a controller: the diffusion and penetration of water and NH_4^+ solution are controlled by swelling and cracking of the coating layer. The permeability of NH_4^+ gone through the coating layer will be decreased if less cracks occur on thicker coating layer surfaces like BCRNF-P6 and BCRNF-P10. This will result in longer N releasing time and lower release rate. In opposite, the release

rate will become higher if more cracks occur on the coating layer surfaces such as BCRNF-P3. If designed properly, the coating layer would be able to control N release in the rate, time, or pattern as desired. Moreover, the BCRNF complex of ammonium sulfate, biochar, and PLA coating layer makes the N release and degradation of BCRNF complex more stable to get along with either microbes or enzymes and resist to higher temperatures with greater moisture content to reduce N volatilization, leaching, or runoff. Therefore, it is possible to develop a good BCRNF product that can synch the N demand time of corn growth while minimizing N lost into environment, eventually, improving NUE of corn production.

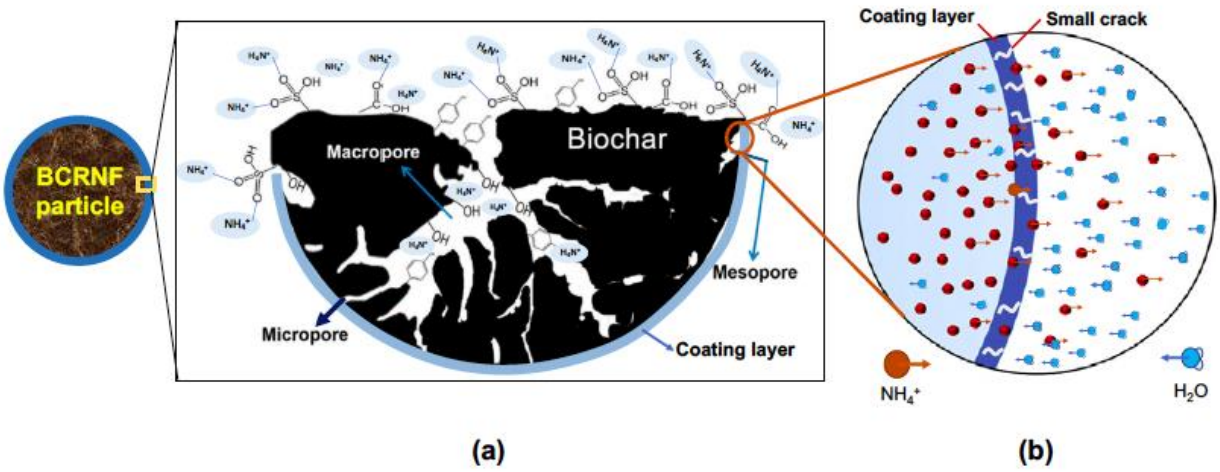

Figure 3.10 Schematic diagram of controllable N releasing mechanism of a BCRNF particle [51]. Note: this figure was created by Dr. Lin Wei and presented in his research report.

3.5 Conclusions

Based on the results and data analysis, some conclusions can be drawn from this study. It is promising to develop an effective biochar-based controlled-release nitrogen fertilizer to improve the ammonium releasing time and rate in both water and soil

environments by integration of biochar absorption and biodegradable polylactic acid coating layer. The polylactic acid concentration of coating layer significantly affected ammonium releasing time and rate. Higher PLA concentrations resulted in longer releasing time at lower N release rates. The releasing time of 70% ammonium of biochar-based controlled-release nitrogen fertilizers coated by 10% and 6% of polylactic acid reached 12 days in water and 25 days under soil conditions. There was no significant difference in ammonium release between the biochar-based controlled-release nitrogen fertilizers coated by 10% and 6% of polylactic acid. It is recommended to use the lower polylactic acid concentration (6%) for coating nitrogen fertilizer to reduce production costs. The biochar produced from corn stover pyrolysis was capable of holding about 14% ammonium not releasing into water. If the biochar-based controlled-release nitrogen fertilizer particles were coated by polylactic acid, the particles could hold at least 16% of ammonium in water or soil. The thermal properties of the biochar-based controlled-release nitrogen fertilizer coated by polylactic acid are stable under 230 °C. It is suggested that further research is necessary to verify the effectiveness of the biochar-based controlled-release nitrogen fertilizer on corn growth; optimize the fabrication process; and perform economic analysis, eventually, develop an affordable, environmentally friendly, and effective biochar-based controlled-release nitrogen fertilizer product that can offer controllable ammonium release to synchronize with the timeline of corn growth to improve nitrogen use efficiency.

Acknowledge

This research was supported by the South Dakota Governor's Office of Economic Development (grant #:POC2020-04) and the USDA NIFA program through the Hatch

Project (No. 3AR652 and 3AH658) of the South Dakota Agricultural Experimental Station.

Note: This chapter 3 was co-author with Dr. Lin Wei, Dr. Kasiviswanathan Muthukumarappan, Abdus Sobhan, and Rachel McDaniel. It was submitted to Journal of Soil Science and Plant Nutrition for publication.

CHAPTER 4: DEVELOP AN ASPHALT-BASED CONTROLLED RELEASE NITROGENOUS FERTILIZER

4.1 Introduction

To attain a more durable N-release pattern than BCRNF discussed in chapter 3, another bio-based nitrogen fertilizer, asphalt-based controlled release nitrogenous fertilizer (ACRNF) was developed. The goal of this study is to develop an asphalt-based controlled release nitrogen fertilizer (ACRNF) to control N release that can synchronize with N demand for corn growth in different stages. Additionally, to achieve the environmentally friendly and low-cost requirements, the bio-asphalt produced from pyrolysis or liquefication of agricultural wastes such as corn stover or sawdust would be individually used as an N carrier in the fabrication of ACRNF. Corn stover and sawdust are agricultural wastes, which are abundant, renewable, cheap, and readily available. They are biodegradable, carbon-neutral, and environmentally friendly. Granular ammonium sulfate would be either mixed or coated with bio-asphalt to fabricate ACRNF to examine their N-release in water in this study. As our best knowledge, this may be the first time that bio-asphalt was used in the fabrication of controlled release fertilizer.

4.2 Materials and methods

4.2.1 Materials

Corn stover (CS) and sawdust (SD) were selected to produce bio-asphalt in this study. The sawdust was purchased from the local store, which was produced by the Rushmore Forest Products Inc. CS feedstock was collected from the experimental farm at South

Dakota State University (SDSU). The CS and SD feedstocks were air-dried and then grounded into powder with particle size generally less than 2 mm by using a hammer mill (Winona Attrition Mill Co.) The moisture contents of feedstocks were analyzed by following the ASTM standard (D4442-07). The particle sizes and distributions of the powder were obtained by using gradient sieves. Ammonium Sulfate (purity > 99.5%) was purchased from the Acros company in the U.S. All chemical reagents were of analytical grade.

4.2.2 Bio-asphalt preparation

Two methods were used to produce bio-asphalt for examining the effects of processing conditions on the N-release patterns of ACRNF. The first bio-asphalt was produced by sawdust pyrolysis, which is a thermal decomposition process that occurs in the absence of oxygen to convert sawdust into three products: liquid bio-oil, non-condensable syngas, and a solid mixture of mineral ash and carbonization residues, so-called bio-char. A pyrolysis reactor was installed in the Ag. & Biosystem Engineering Department at SDSU was used to produce bio-asphalt from the sawdust pyrolysis at 500°C. After sawdust powder was fed into the reactor and pyrolyzed, the bio-oil produced was collected in a glass bottle. When the bio-oil was stored for more than 6 months, a mixture of heavy and long-chain molecules of organic acids, phenols, esters, alcohols, aldehydes, ketones, furans, etc. would precipitate at the bottom of the bottle due to re-polymerization, oxidation, and/or sedimentation. This sediment is called heavy bio-oil or bio-asphalt, which can be easily separated from the bio-oil using phase separation.

The second bio-asphalt was produced by liquefication of the corn stover powder prepared. In a typical run, 60.0 g of 20 mesh corn stover powder and 470 mL of mixture

solvent consisting of water and alcoholic solvents were added to a 1L stainless steel pressure reactor. The reactor was heated in a molten salt bath equipped with a digital temperature controller. The air inside the reactor was released through a release valve when the temperature of the bath reached 170 ^{o}C. After that, the valve was closed, and the bath was heated to 280 ^{o}C for over 30 min. The bath was maintained at this temperature for 5 hours. The mixture produced inside the reactor was transferred to a flask and the solvent was removed by distillation under a reduced pressure (40 mbar) to obtain an asphalt like material, so-called bio-asphalt.

4.2.3 ACRNF preparation

Two types of ACRNF samples were prepared by combining granular ammonium sulfate with the two different bio-asphalts produced from corn stover and sawdust, respectively. The bio-asphalt derived from sawdust pyrolysis was dissolved in acetone for fabricating the first type of ACRNF. Ammonium sulfate was dissolved in deionized water and then impregnated in the mixture of biochar and Kaolin with a ratio of 1:1. The mixture impregnated with Ammonium sulfate was individually blended with the bio-asphalt solution at two ratios: 1:1 and 1:2 to fabricate two ACRNF samples, named ACRNF-1 and ACRNF-2 for later N release experiment. The samples of ACRNF-1 and ACRNF-2 were dried at 80 ^{o}C for 24 hours before the N-release experiment.

The bio-asphalt derived from liquefication of corn stover was used to prepare the second type of ACRNF. To fabricate this ACRNF samples, a small amount (5 g) of the bio-asphalt was further heated up to different temperatures (180 ^{o}C, 200 ^{o}C, 230 ^{o}C, and 240 ^{o}C) under a reduced pressure (40 mbar) for 30 minutes to remove residual solvent and for the material to form additional bonds. Then, the melting bio-asphalts were

individually mixed with ammonium sulfate powder with a ratio of 2:1 in weight. The mixtures were heated to melt in a 5 mL beaker and then poured onto a Teflon surface tray to cool down and then form pellets with dimensions ranging from 3 – 6 mm in sizes. The name of ACRNF was based on asphalt melting temperatures and different sources of bio-asphalt. For example, L-ACRNF-230 means this ACRNF is prepared from the bio-asphalt produced by liquefaction, and the asphalt melting temperature is 230 °C. Similarly, ACRNF180, ACRNF200, ACRNF230, and ACRNF240 also followed this rule of the name in this study.

4.2.4 Characterization of ACRNF

The surface-morphology of ACRNF particles before and after the N release experiment of ACRNF submerging in water were analyzed using a digital microscope (Amscope, UTP200X003MP). The images of ACRNFs' surface-morphology were recorded and then analyzed to examine if any change occurred before and after N release.

4.2.5 Examination of N-release patterns of ACRNF in water

The N-release patterns of ACRNF in water was investigated by the experiment similar to the previous study [40,41]. Firstly, different ACRNF samples were individually submerged into 50 mL of deionized water. Then, the Ammonium (NH_4^+) concentration in the water of each sample was measured every day in 24 hours until the $NH4^+$ concentration having no change for at least 2 days by using an Ammonium ion-selective electrode (ISE) pH meter (Oakton PH 6+). Each measurement was triplicated. The percentage of cumulative NH_4^+ release rate from the samples into the water was calculated using the following equation :

$$\mathrm{Ni} = \frac{Ci*Vi}{Nc*mt} * 100\% \quad (8)$$

Where N_i (%) is the cumulative $NH4^+$ release rate in the water on the i^{th} day (%), C_i (g/L) is the concentration of $NH4^+$ in the water on the i^{th} day, V_i (L) is the volume of the water m_t (g) is the Total mass of the ACRNF sample submerged in the water. N_c (%) is the Percentage of NH_4^+ in the initial ACRNF sample before submerged in the water.

4.3 Results and discussion

4.3.1 Properties of corn stover and sawdust powder

As the corn stover and sawdust feedstocks were dried and ground into powder using the hammer mill, the moisture content and particle size of those feedstocks were determined in our previous study [46]. The results are shown in Table 1. The analysis of those particle size distributions was also carried out and the results are shown as Figures 4.1 and 4.2, respectively. Because of the small particle sizes with large surface areas, the celluloses, hemicelluloses, and lignin in CS or SD powder were fairly easy to be decomposed into bio-oil, biochar and syngas via pyrolysis or liquefication process when they were fed into reactors with the absence of oxygen under high temperature or pressure or both.

Table 4.1 Moisture content and particle size of Feedstocks

Feedstock	Corn Stover	Sawdust
Moisture Content (wt. %)	6.05	7.15
Particle Size < 1mm (wt %)	87	85

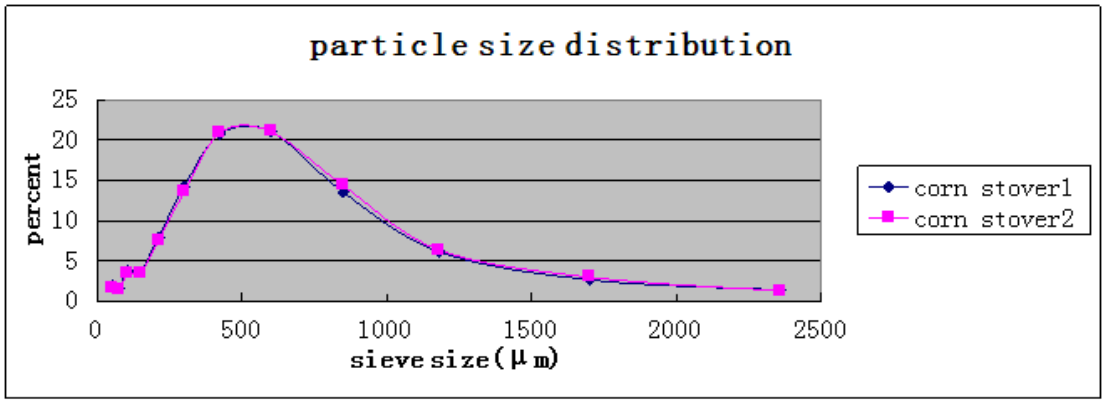

Figure 4.1 Particle size distribution of corn stover powder. (Source from Qu et al [52])

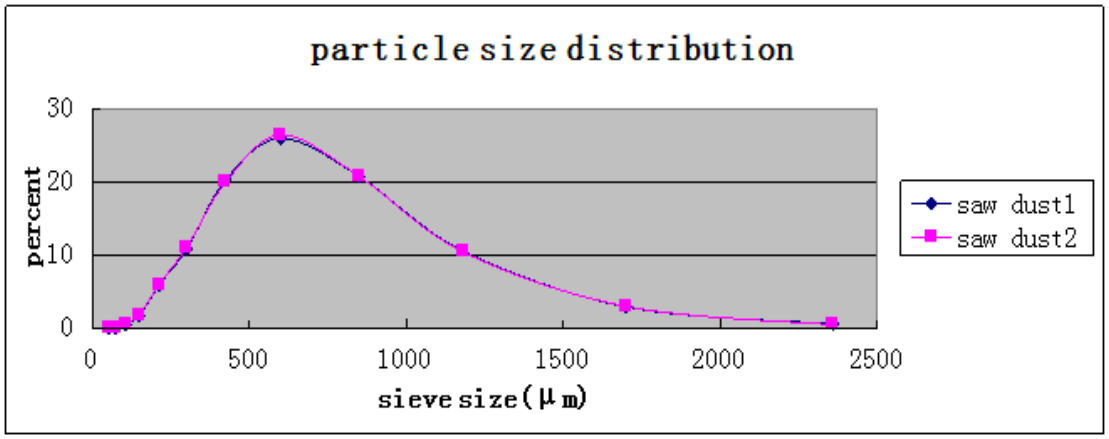

Figure 4.2 Particle size distribution of the pine sawdust. (Source from Qu et al [52])

4.3.2 Properties of Bio-asphalts

The picture of bio-asphalt derived from sawdust pyrolysis is shown in Figure 4.3a. This bio-asphalt has a dark brown color and a very strong odor of tar. According to our previous study[47], its physical properties is shown in table 4.2 and chemical compositions is shown in table 3. The viscosity of the bio-asphalt is very high. The major components of this bio-asphalt included heavy organic acids, phenols, esters, alcohols, aldehydes, ketones, furans, etc., which contain a larger amount of various functional groups, such as C=O, C-O-C, and O-H, etc. These properties indicate that the bio-asphalt has very good potential for use as a binding material in the fabrication of ACRNF, but the effect of these chemical compounds

on corn growth is still unknown. Therefore, more research is needed to identify the suitability of bio-asphalt used in crop production. Figure 4.3b presents the bio-asphalt produced from corn stover by liquefaction method, showing a more compact and smooth surface.

a) Bio-asphalt produced from sawdust pyrolysis

b) Bio-asphalt produced from corn stover liquefaction

Figure 4.3 Bio-asphalt produced from sawdust pyrolysis and corn stover liquefaction.

Table 4.2 Physical properties of bio-asphalt derived from sawdust pyrolysis (Source from Qu et al [53])

Properties	Bio-asphalt
Density (g/ml)	1.14
Viscosity (cp) at 20ºC	8710
pH	3
Moisture content (wt %)	14
Oxygen content (wt %)	33.9

Table 4.3 Major compounds of bio-asphalt derived from sawdust pyrolysis by GC-MS analysis (Source from Qu et al [53])

Retention time (minutes)	Compound names	Area %
4.492	Pyrazole, 1,4-dimethyl-	3.97
5.381	2,4-Octadiyne	2.66
5.999	Bicyclo[2.1.1]hex-2-ene, 2-ethenyl	2.54
6.337	3-Heptyne	1.27

7.916	2-Aminopyrimidine-1-oxide	2.63
9.124	4-(Phenyl)-3,5-dioxaspiro [2.4]heptane,1-carboxylic acid, ethyl ester	2.43
10.966	Phenol, 2-methyl-	2.67
11.95	Ethanone, 1-(1-cyclohexen-1-yl)-	3.86
14.382	Phenol, 3-ethyl-	5.48
15.521	Dodecane	3.92
15.91	Benzofuran, 2,3-dihydro-	3.01
18.473	Benzo[b]thiophene, 2,3-dihydro-3-methyl-	4.94
19.446	2-Cyclohexen-1-ol, 1-methyl-4-(1-methylethyl)-, cis-	1.64
21.426	1-Phenyl-3-methylpenta-1,2,4-trien	1.11
22.055	Eugenol	3.85
26.85	Phenol, 2,6-dimethoxy-4-(2-propeny l)-	2.65
27.062	6-Tridecene, 7-methyl-	1.71
27.377	Diphenylethyne	1.52
28.109	n-Hexadecanoic acid	7.31
28.721	9-Octadecenoic acid, (E)-	9.59
28.796	Bicyclo[2.2.2]oct-5-en-2-one, 7-anti-hydroxy-	4.14
29.088	2-Isopropyl-10-methylphenanthrene	3.02
29.723	1-Phenanthrenecarboxylic acid	8.41
Total		84.33

4.3.3 Surface morphology of ACRNFs using microscopy

The microscope images of ACRNF surface morphology before and after N-release in water are shown in Figure 4.4. The images of original ACRNF samples (Figure 4.4a, c, e, and g) before submerging into water show that there was a smooth and black shining layer on the surface of each particle. This indicates that the surfaces of all ACRNF particles were covered or coated by a layer of bio-asphalt. If the ACRNF samples after N-release were individually named as “used L-ACRNF 180, used P-ACRNF 200, used L-ACRNF 230, and used L-ACRNF 240”, the Figure 4.4b, d, f, and h show that parts or all of the smooth and black shining layers on the used ACRNF particles were disappeared. Instead of the

bio-asphalt cover layers, all surfaces of the used ACRNF particles were brown and rough, distributing with different sizes and numbers of pore structures, depending on the bio-asphalt melting temperatures of fabrication of ACRNF samples. Figure 4.4b, d, and h show that there were fewer numbers but bigger pores on the surfaces when the bio-asphalt melting temperatures were too low (180 ^{o}C and 200 ^{o}C) or too high (240 ^{o}C). In contrast, Figure 4.4f shows that there were much more numbers and smaller pores uniformly dispersed on the surface of the used L-ACRNF 230 particle, which was significantly different from other used ACRNF samples. These different porous structures might result from the swellness and N release patterns of different ACRNF samples when they were fabricated at different bio-asphalt melting temperatures. When the melting bio-asphalt mixed ammonium sulfate powder at lower or higher temperatures, different porous structures would be forming inside the ACRNF particles due to a large number of small bubbles of gas or air generated by chemical reactions or mechanical stirring during the mixing process. The surfaces and pore volumes of the ACRNF particles would be binded or filled by NH_4^+ when bio-asphalt was mixing with ammonium sulfate. Compared to other ACRNF samples, the L-ACRNF 230 has the most numbers and smallest pores structures after the particle was swelling and N-release due to water absorption and desorption, in which the bio-asphalt coated layers were degraded by water hydrolysis.

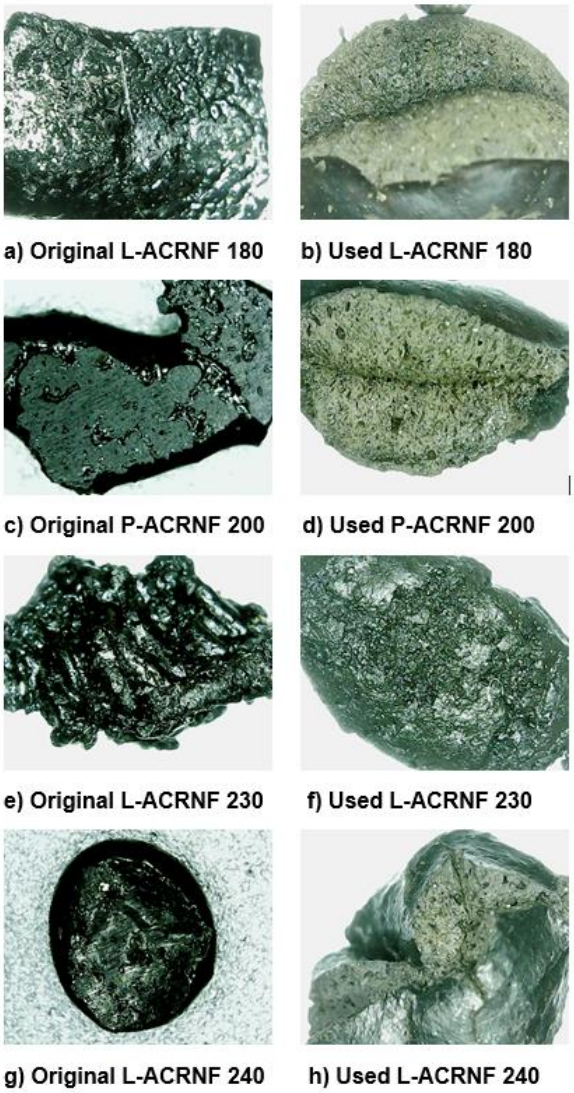

Figure 4.4 Microscope images of ACRNF surface morphology before and after N-release in water.

4.3.4 N−release patterns of ACRNF in water

After the experiment of N release in water was carried out, the results of cumulative N- release rates of different ACRNF samples were shown as Figure 4.5. Compared to the control of pure ammonium sulfate fertilizer releasing more than 90 % of N in the water on the first day, the N-release rates of all ACRNFs were slower. This demonstrates that

bio-asphalt was showing the function of slowing N-release from ACRNF in water as carrier material. This phenomenon may be explained by the specific properties of bio-asphalt produced from hydrothermal liquefication of corn stover. According to a previous study [53], the viscosity of the bio-asphalt was very high. The major components of bio-asphalt included heavy organic acids, phenols, esters, alcohols, aldehydes, ketones, furans, etc., which contain a larger amount of various functional groups, such as C=O, C-O-C, and O-H, etc, [53- 54]. When ammonium sulfate was combined with bio-asphalt, large amounts of NH_4^+ from ammonium sulfate were binding or attracted by these functional groups in a way of ionic bond and hydrogen bond on the surfaces of inside and outside porosity structures of ACRNF particles. However, the strength of these binding bonds is weak. After ACRNF submerged or dissolved in water, these kinds of connections could be broken, and N could be slowly released from the ACRNFS particles due to hydrolysis reactions. The second reason for N slow release from ACRNF was possibly due to the high hydrophobicity of bio-asphalt [55-56]. The strong hydrophobicity can impede water from ACRNF particles and then slow down the ammonium sulfate dissolving and N-nutrients releasing. This hydrophobic property may play an important role in the controlled release of N from ACRNF particles.

Additionally, Figure 4.5 also shows that the N-release patterns of different ACRNF samples were significantly different when they were fabricated at different bio-asphalt melting temperatures. The cumulative N-release rate of L-ACRNF 230 was much slower than that of L-ACRNF 180, P-ACRNF 200, and L-ACRNF 240. This may be caused by specific porosity structure on the surfaces of L-ACRNF 230 particles, as shown in Figure 4.4e. When an ACRNF particle was submerged into water, the water was absorbed by the

ACRNF particle and then penetrated the bio-asphalt coating layer into the particle. The N nutrients on the surfaces or pore volumes of ACRNF were dissolved and then released into the water through the interactions of water absorption and desorption at the early time, which was proved by the fact that all ACRNFs' samples had similar N release rates on the first day. However, after a couple of days, these N release rates were significantly different, depending on the porous structures of ACRNF particles. As mentioned in section 4.3.2, the porous structures were significantly affected by the bio-asphalt melting temperatures. L-ACRNF 230 (Figure 4.4e) has the most numbers and the smallest pores structures. Because of the high hydrophobicity of bio-asphalt and the porous structures, the difficulty of water access to the N nutrients inside ACRNF particles will increase when the pore numbers increase while pore sizes decrease, resulting in lower N-release rate and longer N-release time. This is the reason that L-ACRNF 230 showed the lowest N-release rate and the longest N releasing time in this experiment. The releasing time of 80% N for the L-ACRNF 230 sample was more than 20 days. The N-release pattern of this study was much better than that of not only the conventional ammonium sulfate fertilizer but also the controlled release N fertilizers developed by previous studies. Li and his colleagues developed as controlled release N fertilizer by use of bio-based epoxy coated urea (named EPCU) in 2018 [46]. The best result of their study was the longest N-release time of 80% N was about 10 days, in which just half the time of our L-ACRNF 230 sample. Moreover, compared with the epoxy compounds used in their study, the carrier materials (bio-asphalt) for L-ACRNF 230 fabrication were produced from agricultural waste, which is more economically feasible and environmentally friendly.

In summary, the performance of the ACRNF samples demonstrated the concept of controllable N-release if ammonium sulfate was properly mixing or coating with bio-asphalt by controlling the melting temperature. The properties of the bio-asphalt derived from corn stover liquefication have very good potential for use as a binding material in the fabrication of ACRNF, but the effect of these chemical compounds on corn growth is still unknown. Therefore, more research is needed to identify the suitability of bio-asphalt used in crop production.

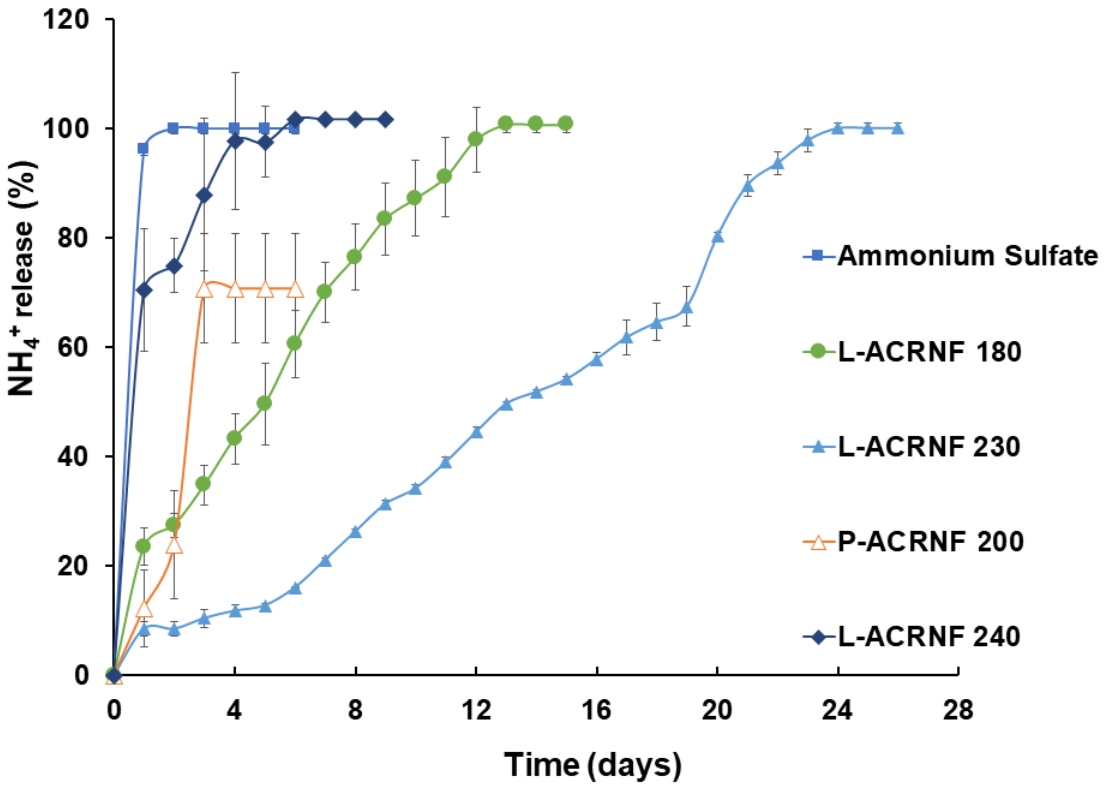

Figure 4.5 N-release of ACRNFs in water.

4.4 Conclusions

Based on the results of this study, it can be concluded that bio-asphalt produced from hydrothermal liquefaction of corn stover can be used as carrier material for the fabrication of control release nitrogen fertilizer. It is feasible to develop a bio-asphalt-based controlled release nitrogen fertilizer (ACRNF) to control N release to synchronize with the N demand of corn growth for improving nitrogen use efficiency. It also found that the N-release patterns of ACRNF were significant affected by the bio-asphalt melting temperatures of the fabrication process. The best melting temperature was 230 ºC, which produced the L-ACRNF 230 sample was able to extend the N-release time of 80% N over 20 days. It is possible to produce controllable and predictable N-release control release fertilizer by use bio-asphalt. Although further research is needed, the ACRNF has shown very promising potential to improve NUE in corn production in the controlled release fertilizer market. Therefore, it is worthy to invest more effort to study the mechanism of ACRNF and move forward to commercialize the technology to the markets.

Acknowledge

This research was supported by the South Dakota Governor's Office of Economic Development (grant #:POC2020-04) and the USDA NIFA program through the Hatch Project (No. 3AR652 and 3AH658) of the South Dakota Agricultural Experimental Station.

Note: This chapter 4 was coauthor with Dr. Lin Wei and Dr. Cheng Zhang. It was published in ASABE 2020 Annual International Meeting, held on July 12–15.

CHAPTER 5: SUMMARY OF RESEARCH

5.1 Conclusions

In this thesis, the studies of activating biochar, biochar-based controlled release nitrogenous fertilizer, and asphalt-based controlled release nitrogenous fertilizer were carried out. It was found that steam-activation is one effective method to activate biochar to improve its physical and chemical properties. The activated biochar has the potential to be used for carbon material applications. This activated biochar can be further upgraded to activation carbon. It can also be combined with nanocelluloses to produce nanofilm. The produced nanocellulose film has high absorption capacity of blue methane as good as activated carbon film.

Moreover, a biochar-based controlled release nitrogenous fertilizer was produced in the studies through coating polylactic acid layers on the particle surfaces of biochar impregnated with ammonium sulfate. The concentrations of polylactic acid solution for coating had significant influences on the nitrogen releasing time and rate. The 10 % of polylactic acid solution coating was able to control 70% of N releasing in water for 12 days, and 25 days in soil environment. The potential of this biochar-based controlled release nitrogenous fertilizer for controlling nitrogen release to synchronizes with the nitrogen demand of corn growth was promising.

Another innovative controlled release nitrogenous fertilizer was also investigated in this thesis. It is possible to produce controlled release nitrogenous fertilizer by mixing bio-asphalt and ammonium sulfate. It was verified that nitrogen release patterns of bio-asphalt-based controlled release nitrogenous fertilizer were significant affected by the bio-asphalt melting temperatures. The best melting temperature for fabrication of the fertilizers was

230 ºC, which was capable of nitrogen releasing time of 80% N over 20 days. Although further research is needed, the bio-asphalt-based controlled release nitrogenous fertilizer shows very promising potential for development of control release nitrogen fertilizers to improve nitrogen use efficiency in corn production.

5.2 Recommendations for the future study

Based on the research results and conclusions, there are some suggestions for the future study.

1) Optimize the process of biochar-based controlled release nitrogenous fertilizer fabrication to further improve the nitrogen releasing time and rate to synchronize with the timeline of nitrogen demand in corn growth and minimize its production costs.
2) Perform greenhouse tests or field trials to examine the effectiveness of biochar-based controlled release nitrogenous fertilizer in real corn production
3) Conduct greenhouse tests or field trials to identify the effectiveness or other effects of bio-asphalt-based controlled release nitrogenous fertilizer on corn production.

REFERENCES

[1] USDA. 2019. Economic Research Service using data from Tennessee Valley Authority (TVA), Association of American Plant Food Control Officials (AAPFCO), and The Fertilizer Institute (TFI), https://www.ers.usda.gov/data-products/fertilizer-use-and-price.aspx

[2] Raun, W. R., & Johnson, G. V. (1999). Improving nitrogen use efficiency for cereal production. *Agronomy journal*, *91*(3), 357-363.

[3] Carpenter, S. R., Caraco, N. F., Correll, D. L., Howarth, R. W., Sharpley, A. N., & Smith, V. H. (1998). Nonpoint pollution of surface waters with phosphorus and nitrogen. *Ecological applications*, *8*(3), 559-568.

[4] Shaviv, A., & Mikkelsen, R. L. (1993). Controlled-release fertilizers to increase efficiency of nutrient use and minimize environmental degradation-A review. *Fertilizer research*, *35*(1-2), 1-12.

[5] Garnett, T., Conn, V., & Kaiser, B. N. (2009). Root based approaches to improving nitrogen use efficiency in plants. *Plant, cell & environment*, *32*(9), 1272-1283.

[6] Pereira, E. I., A. Nogueira, A. R., Cruz, C. C., Guimarães, G. G., Foschini, M. M., Bernardi, A. C., & Ribeiro, C. (2017). Controlled urea release employing nanocomposites increases the efficiency of nitrogen use by forage. *ACS Sustainable Chemistry & Engineering*, *5*(11), 9993-10001.

[7] Abendroth, L.J., R.W. Elmore, M.J. Boyer, & S.K. Marlay. (2011). Corn growth and development. Iowa State University Extension and Outreach, Ames, Iowa.

[8] Bender, R. R., Haegele, J. W., Ruffo, M. L., & Below, F. E. (2013). Transgenic corn rootworm protection enhances uptake and post-flowering mineral nutrient accumulation. *Agronomy Journal*, *105*(6), 1626-1634.

[9] Bender, R. R., Haegele, J. W., Ruffo, M. L., & Below, F. E. (2013). Nutrient uptake, partitioning, and remobilization in modern, transgenic insect-protected maize hybrids. *Agronomy Journal*, *105*(1), 161-170.

[10] Burzaco, J. P., Ciampitti, I. A., & Vyn, T. J. (2014). Nitrapyrin impacts on maize yield and nitrogen use efficiency with spring-applied nitrogen: Field studies vs. meta-analysis comparison. *Agronomy Journal*, *106*(2), 753-760.

[11] Butzen, S. (2011). Nitrogen application timing in corn production. *Crop Insights*, *21*(6).

[12] Ciampitti, I. A., & Vyn, T. J. (2011). A comprehensive study of plant density consequences on nitrogen uptake dynamics of maize plants from vegetative to reproductive stages. *Field Crops Research*, *121*(1), 2-18.

[13] Ciampitti, I. A., & Vyn, T. J. (2012). Physiological perspectives of changes over time in maize yield dependency on nitrogen uptake and associated nitrogen efficiencies: A review. *Field Crops Research*, *133*, 48-67.

[14] Ciampitti, I. A., Murrell, S. T., Camberato, J. J., Tuinstra, M., Xia, Y., Friedemann, P., & Vyn, T. J. (2013). Physiological dynamics of maize nitrogen uptake and partitioning in response to plant density and nitrogen stress factors: II. Reproductive phase. *Crop Science*, *53*(6), 2588-2602.

[15] Ciampitti, I. A., & Vyn, T. J. (2013). Grain nitrogen source changes over time in maize: A review. *Crop Science*, *53*(2), 366-377.

[16] DeBruin, J., Messina, C. D., Munaro, E., Thompson, K., Conlon-Beckner, C., Fallis, L., Sevenich D.M., Gupta, R., & Dhugga, K. S. (2013). N distribution in maize plant as a marker for grain yield and limits on its remobilization after flowering. *Plant breeding*, *132*(5), 500-505.

[17] Duffy, M. (2014). Estimated costs of crop production in Iowa - Ag Decision Maker FM 1712. Iowa State University, Ames, Iowa.

[18] Azeem, B., KuShaari, K., Man, Z. B., Basit, A., & Thanh, T. H. (2014). Review on materials & methods to produce controlled release coated urea fertilizer. *Journal of Controlled Release*, 181, 11-21.

[19] Industry ARC, https://industryarc.com/Report/1262/fertilizers-market-analysis.html

[20] FAO, World fertilizer trends and outlook to 2020. Food and agriculture organization of The United Nations-Rome. (2017). Website: www.fao.org/publications

[21] USDA ERS. Farm resources regions. Visit website on June 15. 30/2019. www.ers.usda.gov

[22] Sempeho, S. I., Kim, H. T., Mubofu, E., & Hilonga, A. (2014). Meticulous overview on the controlled release fertilizers.

[23] Wang, S. L., Heisey, P., Schimmelpfennig, D., & Ball, V. E. (2015). Agricultural productivity growth in the United States: Measurement, trends, and drivers. *Economic Research Service*.

[24] Pereira, E. I., A. Nogueira, A. R., Cruz, C. C., Guimarães, G. G., Foschini, M. M., Bernardi, A. C., & Ribeiro, C. (2017). Controlled urea release employing nanocomposites increases the efficiency of nitrogen use by forage. *ACS Sustainable Chemistry & Engineering*, *5*(11), 9993-10001.

[25] Ding, Y., Liu, Y., Liu, S., Li, Z., Tan, X., Huang, X., Zeng, G., Zhou, L., & Zheng, B. (2016). Biochar to improve soil fertility. A review. *Agronomy for sustainable development*, *36*(2), 36.

[26] Wu, H., Che, X., Ding, Z., Hu, X., Creamer, A. E., Chen, H., & Gao, B. (2016). Release of soluble elements from biochars derived from various biomass feedstocks. *Environmental Science and Pollution Research*, *23*(2), 1905-1915.

[27] Fryda, L., & Visser, R. (2015). Biochar for soil improvement: Evaluation of biochar from gasification and slow pyrolysis. *Agriculture*, *5*(4), 1076-1115.

[28] Ali, S., & Danafar, F. (2015). Controlled-release fertilizers: advances and challenges. *Life Science Journal*, *12*(11), 33-45.

[29] Chen, S., Yang, M., Ba, C., Yu, S., Jiang, Y., Zou, H., & Zhang, Y. (2018). Preparation and characterization of slow-release fertilizer encapsulated by biochar-based waterborne copolymers. *Science of The Total Environment*, *615*, 431-437.

[30] Gwenzi, W., Nyambishi, T. J., Chaukura, N., & Mapope, N. (2018). Synthesis and nutrient release patterns of a biochar-based N–P–K slow-release fertilizer. *International journal of environmental science and technology*, *15*(2), 405-414.

[31] Puga, A. P., Grutzmacher, P., Cerri, C. E. P., Ribeirinho, V. S., & de Andrade, C. A. (2020). Biochar-based nitrogen fertilizers: Greenhouse gas emissions, use efficiency, and maize yield in tropical soils. *Science of The Total Environment*, *704*, 135375.

[32] Wang, Y., Zhang, Y., Li, S., Zhong, W., & Wei, W. (2018). Enhanced methylene blue adsorption onto activated reed-derived biochar by tannic acid. *Journal of Molecular Liquids*, *268*, 658-666.

[33] Sun, K., & chun Jiang, J. (2010). Preparation and characterization of activated carbon from rubber-seed shell by physical activation with steam. *Biomass and bioenergy*, *34*(4), 539-544.

[34] Phanthong, P., Reubroycharoen, P., Hao, X., Xu, G., Abudula, A., & Guan, G. (2018). Nanocellulose: Extraction and application. *Carbon Resources Conversion*, *1*(1), 32-43.

[35] Pereira, E. I., A. Nogueira, A. R., Cruz, C. C., Guimarães, G. G., Foschini, M. M., Bernardi, A. C., & Ribeiro, C. (2017). Controlled urea release employing nanocomposites increases the efficiency of nitrogen use by forage. *ACS Sustainable Chemistry & Engineering*, *5*(11), 9993-10001.

[36] Cen, Z., Wei, L., & Zhang, C. (2020). Develop bio-asphalt-based controlled release nitrogen fertilizers for improving nitrogen use efficiency. In *2020 ASABE Annual International Virtual Meeting* (p. 1). American Society of Agricultural and Biological Engineers.

[37] Atkinson, C. J., Fitzgerald, J. D., & Hipps, N. A. (2010). Potential mechanisms for achieving agricultural benefits from biochar application to temperate soils: a review. *Plant and soil*, *337*(1-2), 1-18.

[38] Downie, A., Crosky, A., & Munroe, P. (2009). Physical properties of biochar. *Biochar for environmental management: Science and technology*, *1*.

[39] Yang, X., Kang, K., Qiu, L., Zhao, L., & Sun, R. (2020). Effects of carbonization conditions on the yield and fixed carbon content of biochar from pruned apple tree branches. *Renewable Energy*, 146, 1691-1699.

[40] Milne, E., Banwart, S. A., Noellemeyer, E., Abson, D. J., Ballabio, C., Bampa, F., ... & Black, H. (2015). Soil carbon, multiple benefits. *Environmental Development*, 13, 33-38.

[41] P Pawar, R., U Tekale, S., U Shisodia, S., T Totre, J., & J Domb, A. (2014). Biomedical applications of poly (lactic acid). *Recent patents on regenerative medicine*, *4*(1), 40-51.

[42] Papangkorn, J., Isaraphan, C., Phinhongthong, S., Opaprakasit, M., & Opaprakasit, P. (2008). Controlled-release material for urea fertilizer from polylactic acid. In *Advanced Materials Research*, 55, 897-900.

[43] Kampeerapappun, P., & Phanomkate, N. (2013). Slow release fertilizer from core-shell electrospun fibers. *Chiang Mai J Sci*, *40*(4), 775-782.

[44] Calcagnile, P., Sibillano, T., Giannini, C., Sannino, A., & Demitri, C. (2019). Biodegradable poly (lactic acid)/cellulose-based superabsorbent hydrogel composite material as water and fertilizer reservoir in agricultural applications. *Journal of Applied Polymer Science*, *136*(21), 47546.

[45] Statista, Monthly export price of polylactic acid in the United States from January 2017 to October 2017. https://www.statista.com/statistics/832246/us-pla-export-price-monthly/

[46] Li, Y., Jia, C., Zhang, X., Jiang, Y., Zhang, M., Lu, P., & Chen, H. (2018). Synthesis and performance of bio-based epoxy coated urea as controlled release fertilizer. *Progress in Organic Coatings*, *119*, 50-56.

[47] Jia, C., Zhang, M., & Lu, P. (2020). Preparation and characterization of polyurethane-/MMT nanocomposite-coated urea as controlled-release fertilizers. *Polymer-Plastics Technology and Materials*, 1-10.

[48] Goodrich, D. C., Faurès, J. M., Woolhiser, D. A., Lane, L. J., & Sorooshian, S. (1995). Measurement and analysis of small-scale convective storm rainfall variability. *Journal of Hydrology*, 173(1-4), 283-308.

[49] Beven, K. J. (2011). Rainfall-runoff modeling: the primer. John Wiley & Sons.

[50] Ye, H. M., Li, H. F., Wang, C. S., Yang, J., Huang, G., Meng, X., & Zhou, Q. (2020). Degradable polyester/urea inclusion complex applied as a facile and environment-friendly strategy for slow-release fertilizer: Performance and mechanism. *Chemical Engineering Journal*, *381*, 122704.

[51] Lee, J., Kim, K. H., & Kwon, E. E. (2017). Biochar as a catalyst. *Renewable and Sustainable Energy Reviews*, *77*, 70-79.

[52] Qu, W., Wei, L., Ma, Z., & Julson, J. (2012). Fast pyrolysis of corn stover and sawdust in a novel reactor. In *2012 Dallas, Texas, July 29-August 1, 2012 (p. 1).* American Society of Agricultural and Biological Engineers.

[53] Qu, W., Wei, L., & Julson, J. (2013). An exploration of improving the properties of heavy bio-oil. *Energy & fuels*, 27(8), 4717-4722.

[54] Yang, X., Mills-Beale, J., & You, Z. (2017). Chemical characterization and oxidative aging of bio-asphalt and its compatibility with petroleum asphalt. *Journal of Cleaner Production*, 142, 1837-1847.

[55] Hill, B., Oldham, D., Behnia, B., Fini, E. H., Buttlar, W. G., & Reis, H. (2018). Evaluation of low temperature viscoelastic properties and fracture behavior of bio-asphalt

mixtures. *International Journal of Pavement Engineering*, 19(4), 362-369.

[56] Zhou, T., Dong, Z., Wang, P., Yang, C., & Luan, H. (2020). Incorporating chemical acids to react with bio-oil: Hydrophobicity improvement and effect on the moisture susceptibility of bio-binder. *Construction and Building Materials*, 255, 119402.